The *nido*-Pb_9^{4-} and the Jahn−Teller Distorted *closo*-Pb_9^{3-} Zintl Anions: Syntheses, X-ray Structures, and Theoretical Studies[1]

Janette Campbell,[2] David A. Dixon,[3] Hélène P. A. Mercier,[2] and Gary J. Schrobilgen*,[2]

Department of Chemistry, McMaster University, Hamilton, Ontario L8S 4M1, Canada, and Central Research and Development Department, Experimental Station, E. I. du Pont de Nemours and Company, Inc., Wilmington, Delaware 19880-0328

Received November 17, 1994[⊗]

The isolation and structural characterization of the nonaplumbide Zintl anion *nido*-Pb_9^{4-} is reported, completing the series of nine-atom homopolyatomic anions of the group IV elements, M_9^{4-} (M = Ge, Sn, Pb). The *nido*-Pb_9^{4-} anion was obtained by extraction of the alloy $KPb_{2.05}$ in ethylenediamine in the presence of a stoichiometric deficit of 2,2,2-crypt (4,7,13,16,21,24-hexaoxa-1,10-diazabicyclo[8.8.8]hexacosane). The K^+(2,2,2-crypt-K^+)$_3$-Pb_9^{4-} salt was obtained as a dark red crystalline compound. The X-ray crystal structure of K^+(2,2,2-crypt-K^+)$_3$-Pb_9^{4-} was determined at −100 °C; it crystallizes in the triclinic system, space group $P\bar{1}$, with two molecules in a unit cell of dimensions a = 15.811(5) Å, b = 16.173(5) Å, c = 20.180(6) Å, α = 98.60(3)°, β = 104.59(2)°, and γ = 118.32(2)° with R = 0.0673 for 11 833 observed ($I > 2\sigma(I)$) reflections. The use of an excess of 2,2,2-crypt allowed the isolation of (2,2,2-crypt-K^+)$_3$$Pb_9^{3-}$ containing the Pb_9^{3-} anion which proved to be identical to the recently reported Pb_9^{3-} anion in (2,2,2-crypt-K^+)$_3$$Pb_9^{3-}$·0.5en. The (2,2,2-crypt-K^+) salts contain the nine-atom homopolyatomic cluster anions *nido*-Pb_9^{4-} and *closo*-Pb_9^{3-} which have monocapped square antiprismatic (C_{4v} point symmetry) and distorted tricapped trigonal prismatic (C_{2v} point symmetry) geometries, respectively. Uncomplexed potassium atoms bridge the waist edges of the Pb_9^{4-} anion in the K^+(2,2,2-crypt-K^+)$_3$$Pb_9^{4-}$ salt forming infinite −K−(Pb$_9$)−K−(Pb$_9$)−K− chains. The structures of *nido*-Pb_9^{4-} and related group IV analogs are predicted by Wade's rules and possess $2n + 4$ skeletal electrons whose structures are monocapped square antiprisms of approximate C_{4v} point symmetry derived from 10-vertex polyhedra. The observed geometry of the *closo*-Pb_9^{3-} can also be accommodated by Wade's rules and is regarded as a *closo*-structure which is Jahn−Teller distorted to C_{2v}-symmetry. Results from local and nonlocal density functional calculations show that for Pb_9^{4-} and Pb_9^{3-}, the C_{4v} and C_{2v} symmetries are true minima and are in agreement with their experimentally determined structures.

Introduction

The discovery of polyatomic anions of the heavy post-transition elements in 1891 is attributed to Joannis[4] and include the first reports of alkali metal plumbides. He observed that the reaction of excess lead with alkali metals in liquid ammonia produced an intense green-colored solution and the intermetallic phases precipitated from these solutions had the compositions $NaPb_4 \cdot 2NH_3$[4] and KPb_2.[5] In 1907, Kraus[6] reported a green sodium/lead solution in liquid ammonia which behaved as an electrolyte and which plated out lead at the anode when a current was passed through this solution. Similar behavior was observed for sodium/tin solutions in liquid ammonia. Kraus proposed that the sodium/lead solution contained the Na^+ and Pb_2^- ions since 2 mol of lead atoms per Faraday were transferred from the anode to the cathode. In 1917, Smyth[7] observed that, under electrolytic conditions, 2.26 mol of Pb per Faraday plated out on the anode and led him to suggest that a mixture of Pb_2^- and Pb_3^- anions was responsible for the green color of sodium/lead solutions. On the basis of these observations, Kraus[8] concluded that the anion responsible for the green color of these sodium/lead ammonia solutions was, in fact, Pb_9^{4-}.

In the 1930's, Zintl and co-workers[9-12] determined, by potentiometric titrations of sodium in liquid ammonia with PbI_2, that the compositions of the sodium/lead compounds were Na_4Pb_x (x = 6.89−7.02) and Na_4Pb_y (y = 8.86−9.11). Zintl and Harder[10] also attempted to isolate a crystalline salt from solutions obtained by extraction of the alloy Na_4Pb_9 in liquid ammonia by evaporation of the solvent. This attempt, however, resulted in the formation of an amorphous amine complex according to eq 1, which lost ammonia to yield a metallic compound which

$$4Na^+(am) + Pb_9^{4-}(am) + 4nNH_3(l) \rightarrow [Na(NH_3)_n]_4Pb_9(s) \quad (1)$$

was identical to the starting alloy (eq 2). Zintl showed by X-ray

$$[Na(NH_3)_n]_4Pb_9(s) \rightarrow Na_4Pb_9(s) + 4nNH_3(g) \quad (2)$$

powder diffraction that the starting alloy, Na_4Pb_9, consisted of a cubic atomic lattice without any cluster units and proposed the existence of a short lived intermediate phase between the amine $[Na(NH_3)_n]_4Pb_9$ and the alloy Na_4Pb_9 consisting of discrete Pb_9^{4-} anions and Na^+ cations.

Kummer and Diehl[13] isolated the first solid derivative of a Zintl anion in 1970, namely, $Na_4(en)_7Sn_9$ (en = ethylenedi-

⊗ Abstract published in *Advance ACS Abstracts,* October 15, 1995.
(1) Presented at the 207th ACS National Meeting, San Diego, CA, March 13−17, 1994; abstract no. 349.
(2) McMaster University.
(3) E. I. du Pont de Nemours and Co., Inc. DuPont Contribution No. 7052.
(4) Joannis, A. *C. R. Hebd. Seances Acad. Sci.* **1891**, *113*, 795.
(5) Joannis, A. *C. R. Hebd. Seances Acad. Sci.* **1892**, *114*, 587.
(6) Kraus, C. A. *J. Am. Chem. Soc.* **1907**, *29*, 1571.
(7) Smyth, F. H. *J. Am. Chem. Soc.* **1917**, *39*, 1299.
(8) Kraus, C. A. *J. Am. Chem. Soc.* **1922**, *44*, 1216.
(9) Zintl, E.; Goubeau, J.; Dullenkopf, W. *Z. Phys. Chem., Abt. A* **1931**, *154*, 1.
(10) Zintl, E.; Harder, A. *Z. Phys. Chem., Abt. A* **1931**, *154*, 47.
(11) Zintl, E.; Dullenkopf, W. *Z. Phys. Chem., Abt. B* **1932**, *16*, 183.
(12) Zintl, E.; Kaiser, H. *Z. Anorg. Allg. Chem.* **1933**, *211*, 113.
(13) Kummer, D.; Diehl, L. *Angew. Chem., Int. Ed. Engl.* **1970**, *9*, 895.

0020-1669/95/1334-5798$09.00/0

amine), and incompletely characterized it by X-ray crystallography. More recently, Corbett and co-workers[14] have used 2,2,2-crypt as a sequestering agent for the alkali metal cations in order to prevent electron transfer from the anions to the cations. The use of 2,2,2-crypt has allowed the isolation and X-ray structural characterization of a number of heteropolyatomic naked cluster anions of groups III and IV [Sn_8Tl^{3-}, Sn_9Tl^{3-}][15] and homopolyatomic naked cluster anions of group IV [Ge_9^{m-} (m = 2,[16] 3,[17] and 4[16]), Ge_{10}^{2-},[17] Ge_4^{2-},[18] Sn_9^{m-} (m = 3,[19] 4[20,21]), Sn_5^{2-},[22] Sn_4^{2-},[18] and Pb_5^{2-} [22]] and group V [Sb_4^{2-},[23] Bi_4^{2-} [24]]. Attempts to isolate the 2,2,2-crypt-M^+ (M = K and/or Na) salt of the Pb_9^{4-} anion by Corbett and co-workers[22] resulted in the unexpected isolation of the trigonal bipyramidal Pb_5^{2-} anion (D_{3h} point symmetry) in (2,2,2-crypt-Na^+)$_2Pb_5^{2-}$, which was, until recently, the only homopolyatomic lead anion to have been structurally characterized by X-ray crystallography. Although the NMR characterization of the Pb_5^{2-} anion has been alluded to,[25] no unambiguous characterization in solution by ^{207}Pb NMR spectroscopy has been reported, whereas the Pb_9^{4-} anion and its mixed analogs $Sn_{9-x}Pb_x^{4-}$ (x = 0−9), $Sn_{9-x}Ge_x^{4-}$ (x = 0−8), $Sn_{8-x}Pb_xTl^{5-}$ (x = 0−8) and Sn_8Tl^{5-} have been identified in en solutions by ^{207}Pb, ^{205}Tl and ^{119}Sn NMR spectroscopy.[26-30] The detailed structural characterization of Pb_9^{4-} and its mixed nine-atom analogs by NMR spectroscopy is prevented by their fluxionality. Fluxionality of these nine-atom cluster anions is attributed to rapid intramolecular interconversion between the *nido*-C_{4v} and the *closo*-D_{3h} structures by means of a C_{2v} transition state.[31]

The structure of the Pb_9^{4-} anion has been the subject of speculation from the time it was first identified. Zintl,[9] who formulated Pb_9^{4-} as $Pb_8{\cdot}Pb^{4-}$, based his structural proposal on structures of polysulfides, namely $Na_2S(S)_x$, leading to the interpretation that the lead anion may consist of a central metal anion Pb^{4-} symmetrically bonded to eight neutral lead atoms giving a $Pb_8{\cdot}Pb^{4-}$ cube. Pauling[32] apparently also speculated early on about the structure of the Pb_9^{4-} anion and also suggested that Pb_9^{4-} consisted of a Pb^{4-} anion body centered in a Pb_8 cube and may have been influenced by the formulation originally proposed by Zintl. In view of the existence of Pb_4 tetrahedra in NaPb, Marsh and Shoemaker[33] suggested that the Pb_9^{4-} anion consisted of three Pb_4 tetrahedra sharing vertices to give essentially a tricapped trigonal prismatic geometry. Later, on the basis of the structure of the *closo*-Bi_9^{5+} cation (tricapped trigonal prismatic, D_{3h} point symmetry) in $(Bi_9^{5+})_2(BiCl_5^{2-})_4(Bi_2Cl_8^{2-})$,[34] Britton[35] suggested that since Pb_9^{4-} is isoelectronic with Bi_9^{5+}, it should also be isostructural. However, a second structure of the Bi_9^{5+} cluster in $Bi_{12}Cl_{14}$[36] was shown to have essentially C_{4v} point symmetry, i.e., a *nido*-structure. The tin and germanium nine-atom clusters Sn_9^{4-} and Ge_9^{4-}, isovalent with Pb_9^{4-}, have *nido*-structures based on ten-vertex polyhedra with one-vertex unoccupied to give monocapped square antiprismatic (C_{4v}) geometries. Subsequent to our initial report of the crystal structures of the Pb_9^{3-} and Pb_9^{4-} anions[1] and submission of the present paper, a communication describing the Pb_9^{3-} anion recently appeared in this journal.[37] The odd electron M_9^{3-} (M = Ge, Sn, Pb) clusters are found to be *closo*-C_{2v} or -D_{3h} polyhedra.

Interestingly, the Pb_9^{4-} anion, the first polyanion discovered by Zintl's group, has never been isolated and structurally characterized even though it has been observed in the recent crystal structure of (2,2,2-crypt-K^+)$_4$Cr(CO)$_3Pb_9^{4-}$,[38] where the anion can be described as a square antiprism of lead atoms having Cr and Pb atoms in capping positions. The isolation of the Pb_9^{3-} and the Pb_9^{4-} anions, while of historical note, also completes both series of group IV nine-atom cluster anions, thereby allowing for a fuller understanding of the nature of bonding and factors affecting structural differences observed among naked metal clusters.

The present work reports the preparation and the structural characterization in the solid state of two Pb_9 cluster anions in the salts K^+(2,2,2-crypt-K^+)$_3Pb_9^{4-}$ and (2,2,2-crypt-K^+)$_3Pb_9^{3-}$.[39] The latter structure is compared to that recently published by Fässler and Hunziker.[37] Density functional calculations at the local (LDFT) and nonlocal (NLDFT) levels have been done to establish their theoretical optimized geometries and are compared with the experimental findings.

Results and Discussion

Syntheses of the Pb_9 Cluster Anions. The experimental approach involved the synthesis of the binary alloy $KPb_{2.05}$ by fusion of the elements and extraction of the powdered alloy in en in the presence of 2,2,2-crypt. The alloy composition used is that reported by Joannis[5] and is a stable phase in the K−Pb phase diagram reported by Shoikhet and co-workers.[40] The present study shows that by using the same starting alloy and en as a solvent, the nature of the anion in solution varies depending on whether or not 2,2,2-crypt is used in stoichiometric excess or deficit with respect to the amount of potassium in the alloy.

The ^{207}Pb NMR spectra of the brown solutions obtained by extraction of $KPb_{2.05}$ in en in the absence and presence of 2,2,2-crypt (K^+: 2,2,2-crypt = 2:1) gave rise to a singlet at −4111 ppm ($\nu_{1/2}$ = 23 Hz) which is in agreement with the chemical shift previously reported for solutions of Pb_9^{4-} anion (−4098 ppm) obtained by extraction of the KPb_2 alloy in en.[29] The

(14) Corbett, J. D.; Adolphson, D. G.; Merryman, D. J.; Edwards, P. A.; Armatis, F. J. *J. Am. Chem. Soc.* **1975**, *97*, 6267.
(15) Burns, R. C.; Corbett, J. D. *J. Am. Chem. Soc.* **1982**, *104*, 2804.
(16) Belin, C. H. E.; Corbett, J. D.; Cisar, A. *J. Am. Chem. Soc.* **1977**, *99*, 7163.
(17) (a) Angilella, V.; Belin, C. *J. Chem. Soc., Faraday Trans.* **1991**, *87*, 203. (b) Belin, C.; Mercier, H.; Angilella, V. *New. J. Chem.* **1991**, *15*, 931.
(18) Critchlow, S. C.; Corbett, J. *J. Chem. Soc., Chem. Commun.* **1981**, 236.
(19) Critchlow, S. C.; Corbett, J. D. *J. Am. Chem. Soc.* **1983**, *105*, 5715.
(20) Corbett, J. D.; Edwards, P. A. *J. Am. Chem. Soc.* **1977**, *99*, 3313.
(21) Burns, R. C.; Corbett, J. D. *Inorg. Chem.* **1985**, *24*, 1489.
(22) Edwards, P. A.; Corbett, J. D. *Inorg. Chem.* **1977**, *16*, 903.
(23) Critchlow, S. C.; Corbett, J. D. *Inorg. Chem.* **1984**, *23*, 770.
(24) Cisar, A.; Corbett, J. D. *Inorg. Chem.* **1977**, *16*, 2482.
(25) Wilson, W. L. Ph.D. Thesis.
(26) Rudolph, R. W.; Wilson, W. L.; Parker, F.; Taylor, R. C.; Young, D. C. *J. Am. Chem. Soc.* **1978**, *100*, 4629.
(27) Rudolph, R. W.; Taylor, R. C.; Young, D. C. In *Fundamental Research in Homogeneous Catalysis*; Tsutsui, M., Ed.; Plenum Press: New York, 1979; pp 997−1005.
(28) Pons, B. S.; Santure, D. J.; Taylor, R. C.; Rudolph, R. W. *Electrochem. Acta.* **1981**, *26*, 365.
(29) Wilson, W. L.; Rudolph, R. W.; Lohr, L. L.; Taylor, R. C.; Pyykkö, P. *Inorg. Chem.* **1986**, *25*, 1535.
(30) Rudolph, R. W.; Wilson, W. L. *J. Am. Chem. Soc.* **1981**, *103*, 2480.
(31) Guggenberger, L. J.; Muetterties, E. L. *J. Am. Chem. Soc.* **1976**, *98*, 7221.
(32) Pauling, L. Private communication to G. J. Schrobilgen, June, 1985.
(33) Marsh, R. E.; Shoemaker, D. P. *Acta. Crystallogr.* **1953**, *6*, 197.
(34) Friedman, R. M.; Corbett, J. D. *Inorg. Chem.* **1973**, *12*, 1134.
(35) Britton, D. *Inorg. Chem.* **1964**, *3*, 305.
(36) Hershaft, A.; Corbett, J. D. *Inorg. Chem.* **1963**, *2*, 979.
(37) Fässler, T. F.; Hunziker, M. *Inorg. Chem.* **1994**, *33*, 5380; this paper also reports the structure of (2,2,2-crypt-K^+)$_3Ge_9^{3-}{\cdot}$0.5en.
(38) Eichhorn, B. W.; Haushalter, R. C. *J. Chem. Soc., Chem. Commun.* **1990**, 937.
(39) **(2,2,2-crypt-K^+)$_3Pb_9^{3-}$:** $C_{54}H_{108}K_3N_6O_{18}Pb_9$ (fw = 3111.47), crystallizes in the triclinic system, space group $P\bar{1}$, with a = 15.018(3) Å, b = 16.378(3) Å, c = 20.520(4) Å, α = 92.73(2)°, β = 96.86(2)°, γ = 111.54(1)°, V = 4638(2) Å^3, and D_{calc} = 2.228 g cm^{-3} for Z = 2. Ag Kα radiation (λ = 0.56086 Å, μ(Ag Kα) = 89.9 cm^{-1}) was used.
(40) Shoikhet, D. N.; Morachevskii, A. G.; Alabyshev, A. F. *Russ. J. Inorg. Chem. (Engl. Transl.)* **1959**, *4*, 728.

Table 1. Summary of Crystal Data and Refinement Results for $K^+(2,2,2\text{-crypt-}K^+)_3Pb_9^{4-}$

chemical formula	$C_{54}H_{108}K_4N_6O_{18}Pb_9$	V (Å^3)	4171(2)
color	dark red	Z	2
space group	$P\bar{1}$	fw	3150.57
a (Å)	15.811(5)	ρ_{calcd} (g cm^{-3})	2.426
b (Å)	16.173(5)	T (°C)	-100
c (Å)	20.180(6)	μ (cm^{-1})	100.3
α (deg)	98.60(3)	λ (Å)	0.560 86
β (deg)	104.59(2)	final agreement factors[a]	$R = 0.0673$
γ (deg)	118.32(2)		$R = 0.0447$

[a] $R = \sum||F_o| - |F_c||/\sum|F_o|$. $R_w = \sum(|F_o| - |F_c|)w^{1/2}|/\sum(|F_o|w^{1/2})$ where $w = 1/[\sigma^2(F) + 0.000005F^2]$.

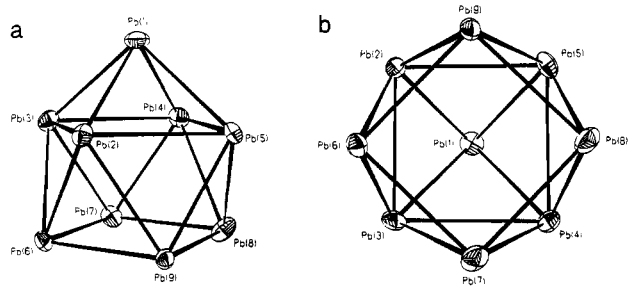

Figure 1. Two ORTEP views of the *nido*-Pb_9^{4-} anion in $K^+(2,2,2\text{-crypt-}K^+)_3Pb_9^{4-}$ showing the monocapped square antiprismatic geometry (a) viewed along a pseudo-C_3-axis and (b) viewed along the C_4-axis. Thermal ellipsoids are shown at the 50% probability level.

observation of a single narrow ^{207}Pb resonance indicates that all lead environments of the Pb_9 cluster are magnetically and chemically equivalent on the NMR time scale owing to a rapid intramolecular exchange (fluxional) process which prevents structural characterization in solution by NMR spectroscopy, and suggests that the solution is essentially free of paramagnetic Pb_9^{3-} (*vide infra*).

No ^{207}Pb NMR signal could be detected for the emerald green solution obtained by extraction of $KPb_{2.05}$ in en in the presence of an excess of 2,2,2-crypt (K^+: 2,2,2-crypt = 1:1.2), even though the intense green color has generally been associated with the Pb_9^{4-} anion.[10] Interestingly, this color was observed for Na/Pb solutions in liquid ammonia.[10] No resonances were observed from +2000 to −5500 ppm, the region where the ^{207}Pb resonances of lead clusters are normally expected to occur.[26-30] Our inability to observe a signal(s) is consistent with the presence of a paramagnetic species in solution (see **X-ray Crystal Structure of $(2,2,2\text{-crypt-}K^+)_3Pb_9^{3-}$**). An NMR signal corresponding to the Pb_5^{2-} anion could not be detected in either of these solutions.

All solutions, whether containing a stoichiometric deficit or an excess of 2,2,2-crypt, gave rise to crystalline material having three distinct morphologies: dark red needle-shaped crystals, whose morphology resembled the morphologies previously described for $(2,2,2\text{-crypt-}K^+)_2Pb_5^{2-}$ and $(2,2,2\text{-crypt-}Na^+)_2Pb_5^{2-}$,[22] which failed to diffract, and hexagonal and parallelepiped shaped crystal morphologies whose unit cells were unknown. Consequently, the latter crystals were characterized by X-ray crystallography and shown to be $K^+(2,2,2\text{-crypt-}K^+)_3Pb_9^{4-}$ and $(2,2,2\text{-crypt-}K^+)_3Pb_9^{3-}$, respectively.

Structural Characterization by X-ray Crystallography. Details of the data collection parameters and other crystallographic information are given in Table 1 for Pb_9^{4-}. The final atomic coordinates and equivalent isotropic thermal parameters for the non-hydrogen atoms are summarized in Table 2 for Pb_9^{4-}. The most significant contacts and angles in the *nido*-Pb_9^{4-} anion as well as the long contact distances in the $K^+Pb_9^{4-}$ unit are listed in Table 3. Analogous data for the Pb_9^{3-} anion are given in Supporting Tables 7, 8, and 10. Important contacts and dihedral angles required for symmetry assessment of the

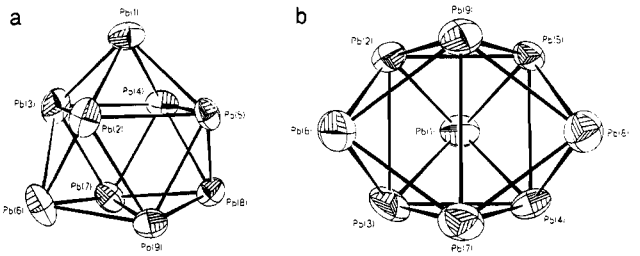

Figure 2. Two ORTEP views of the *closo*-Pb_9^{3-} anion in $(2,2,2\text{-crypt-}K^+)_3Pb_9^{3-}$ showing the tricapped trigonal prismatic geometry (a) viewed along the C_3-axis and (b) viewed along the C_2-axis. Thermal ellipsoids are shown at the 50% probability level.

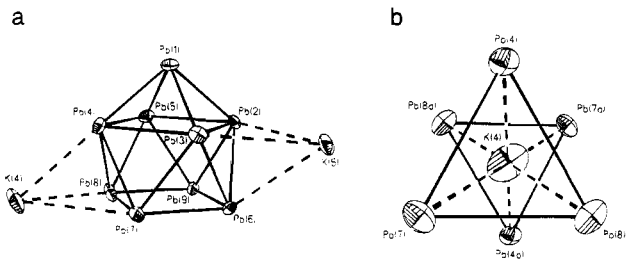

Figure 3. (a) Independent $K^+Pb_9^{4-}$ unit in $K^+(2,2,2\text{-crypt-}K^+)_3Pb_9^{4-}$ showing the long contacts to the uncomplexed bridging K(4) and K(5) atoms. (b) Environment around one of the uncomplexed potassium atoms. Thermal ellipsoids are shown at the 50% probability level.

Pb_9^{4-} and Pb_9^{3-} structures are listed in Table 4, and Pb_9^{3-} structural parameters referred to in the discussion are taken from our independent structure determination of $(2,2,2\text{-crypt-}K^+)_3Pb_9^{3-}$. Figures 1 and 2 illustrate, from two different perspectives, the geometries of the *nido*-Pb_9^{4-} and *closo*-Pb_9^{3-} anions, respectively, and the numbering scheme used throughout the paper for all nine-atom clusters.

In both compounds, the structures of the $(2,2,2\text{-crypt-}K^+)$ cations are similar to those determined previously for symmetry unconstrained units in $(2,2,2\text{-crypt-}K^+)_3As_{11}^{3-}$,[41] $(2,2,2\text{-crypt-}K^+)_3Sn_9^{3-}$,[19] and $(2,2,2\text{-crypt-}K^+)_3P(C_6H_5)_3Ge_9^{3-}$ [17] with average K−O and K−N distances of 2.84(6) and 2.98(4) Å for $K^+(2,2,2\text{-crypt-}K^+)_3Pb_9^{4-}$ and 2.8(2) and 2.9(1) Å for $(2,2,2\text{-crypt-}K^+)_3Pb_9^{3-}$, respectively. A complete list of bond lengths and angles in the $(2,2,2\text{-crypt-}K^+)$ cations is provided in Supporting Table 11.

X-ray Crystal Structure of $K^+(2,2,2\text{-crypt-}K^+)_3Pb_9^{4-}$. The crystal structure of $K^+(2,2,2\text{-crypt-}K^+)_3Pb_9^{4-}$ consists of six cryptated potassium cations and two nine-lead atom cluster anions bridged by two noncryptated potassium cations. The most interesting feature of the structure is the Pb_9^{4-} anion (Figure 1), which was found to have the monocapped square antiprismatic geometry (C_{4v} point symmetry).

The presence of uncomplexed potassium cations K(4) and K(5) makes this structure isostructural with that of the tin analog, $(2,2,2\text{-crypt-}K^+)_3(KSn_9^{3-})$.[21] The potassium atoms K(4) and K(5) are positioned on the centers of symmetry 0,0,0 and 0,0,$^1/_2$ and bridge the waist edges of the cluster as shown in Figure 3a. Each uncomplexed potassium atom has four nearest neighbor lead atoms at 3.498(1)−3.691(1) Å (average 3.643(2) Å) with two longer K···Pb distances at 4.057(2) and 4.173(2) Å, completing a trigonal antiprism about each potassium atom (Figure 3b). The K···Pb distances may be compared with the K···Pb distances found in the intermetallic phase KPb_2 (3.91 Å).[42] Thus, the potassium-lead distances in the present work appear to be in the normal range except for the somewhat shorter K(4)···Pb(8) distance (3.498(1) Å). The four shortest K···Sn

(41) Belin, C. H. E. *J. Am. Chem. Soc.* **1980**, *102*, 6036.
(42) Gilde, V. D. *Z. Anorg. Allg. Chem.* **1956**, *284*, 142.

Table 2. Atomic Coordinates ($\times 10^4$) and Equivalent Isotropic Displacement Coefficients ($Å^2 \times 10^3$) for $K^+(2,2,2\text{-crypt-}K^+)_3Pb_9^{4-}$

	x	y	z	U(eq)		x	y	z	U(eq)
Pb(1)	12168(1)	9804(1)	3228(1)	28(1)	C(207)	6821(14)	1437(12)	−1620(9)	25(4)
Pb(2)	10227(1)	8598(1)	3533(1)	20(1)	C(208)	7400(14)	1251(12)	−1002(9)	29(5)
Pb(3)	11039(1)	10889(1)	3436(1)	25(1)	N(209)	7869(11)	2018(9)	−320(7)	21(3)
Pb(4)	11331(1)	10240(1)	1871(1)	26(1)	C(210)	8764(14)	2939(12)	−300(9)	29(5)
Pb(5)	10458(1)	7898(1)	1992(1)	26(1)	C(211)	9050(14)	3811(12)	273(9)	26(4)
Pb(6)	8729(1)	9312(1)	3007(1)	21(1)	O(212)	8285(9)	4038(8)	118(6)	24(3)
Pb(7)	9438(1)	10342(1)	1904(1)	29(1)	C(213)	8591(13)	4971(11)	614(9)	22(4)
Pb(8)	9077(1)	8401(1)	989(1)	31(1)	C(214)	7732(14)	5122(13)	480(10)	31(5)
Pb(9)	8361(1)	7399(1)	2077(1)	19(1)	O(215)	6903(10)	4351(9)	614(7)	37(3)
K(5)	10000	10000	5000	42(4)	C(216)	6090(15)	4547(13)	585(10)	35(5)
K(4)	10000	10000	0	58(4)	C(217)	5256(16)	3759(13)	704(10)	40(5)
K(1)	6122(3)	3957(3)	6772(2)	24(2)	C(218)	4017(14)	2006(12)	399(9)	30(5)
N(100)	4586(11)	2318(10)	5347(7)	25(4)	C(219)	4577(15)	1777(13)	997(10)	33(5)
C(101)	4397(14)	2797(12)	4798(9)	30(5)	O(220)	5111(9)	1377(8)	736(6)	29(3)
C(102)	5321(14)	3700(12)	4843(9)	28(4)	C(221)	5694(15)	1167(13)	1293(10)	34(5)
O(103)	5734(9)	4450(8)	5522(6)	23(3)	C(222)	6195(14)	672(12)	972(9)	29(4)
C(104)	6563(14)	5349(12)	5519(9)	32(5)	O(223)	6908(9)	1371(8)	731(6)	27(3)
C(105)	6930(16)	6140(13)	6218(10)	39(5)	C(224)	7393(14)	909(12)	449(10)	31(5)
O(106)	7416(10)	5899(8)	6805(6)	31(3)	C(225)	8206(14)	1652(12)	272(9)	30(5)
C(107)	7848(17)	6704(14)	7475(10)	49(6)	K(3)	7595(3)	3331(3)	3678(2)	20(2)
C(108)	8379(18)	6444(15)	8072(12)	57(7)	N(300)	7341(12)	1561(11)	4024(8)	32(4)
N(109)	7679(12)	5579(11)	8215(8)	34(4)	C(301)	7411(15)	938(13)	3437(10)	35(5)
C(110)	8227(16)	5196(14)	8627(10)	41(5)	C(302)	8318(16)	1523(14)	3222(11)	47(6)
C(111)	8587(16)	4659(14)	8196(10)	42(6)	O(303)	8180(10)	2197(9)	2910(7)	34(3)
O(112)	7683(10)	3784(9)	7637(6)	33(3)	C(304)	8930(15)	2669(13)	2630(10)	36(5)
C(113)	8046(15)	3300(12)	7246(10)	34(5)	C(305)	8764(15)	3363(13)	2293(10)	35(5)
C(114)	7142(15)	2338(13)	6742(10)	36(5)	O(306)	8845(9)	4103(8)	2850(6)	21(3)
O(115)	6503(10)	2485(8)	6191(6)	29(3)	C(307)	8798(15)	4857(12)	2606(9)	32(5)
C(116)	5599(14)	1559(12)	5727(9)	32(5)	C(308)	8787(14)	5529(12)	3164(9)	29(5)
C(117)	5019(14)	1737(12)	5120(9)	26(4)	N(309)	7879(11)	5119(9)	3364(7)	21(3)
C(118)	3625(14)	1649(12)	5443(9)	29(5)	C(310)	7989(14)	5825(12)	3974(9)	28(4)
C(119)	3292(14)	2223(12)	5865(9)	29(5)	C(311)	8756(14)	5983(11)	4675(9)	23(4)
O(120)	4042(9)	2741(8)	6579(6)	27(3)	O(312)	8408(9)	5084(8)	4825(6)	25(3)
C(121)	3701(15)	3254(13)	6982(9)	34(5)	C(313)	9091(14)	5227(12)	5513(9)	28(4)
C(122)	4437(14)	3705(12)	7749(9)	31(5)	C(314)	8663(14)	4245(12)	5648(9)	27(4)
O(123)	5421(10)	4496(8)	7812(6)	29(3)	O(315)	8598(9)	3522(8)	5138(6)	24(3)
C(124)	6079(15)	4879(13)	8542(10)	38(5)	C(316)	8280(14)	2616(12)	5319(9)	29(5)
C(125)	7073(16)	5779(14)	8611(11)	44(6)	C(317)	8147(14)	1845(12)	4728(9)	29(5)
K(2)	6294(3)	2404(3)	−89(2)	21(2)	C(318)	6354(14)	997(13)	4057(10)	33(5)
N(200)	4730(11)	2796(9)	177(7)	20(3)	C(319)	5459(14)	840(12)	3450(9)	28(4)
C(201)	4112(14)	2773(12)	−516(9)	27(4)	O(320)	5571(9)	1782(7)	3465(5)	19(3)
C(202)	3797(13)	1933(12)	−1184(9)	23(4)	C(321)	4724(14)	1636(12)	2879(9)	26(4)
O(203)	4704(9)	2105(8)	−1275(6)	26(3)	C(322)	4832(14)	2606(11)	2882(9)	25(4)
C(204)	4402(14)	1402(12)	−1959(9)	27(4)	O(323)	5799(9)	3253(7)	2835(5)	18(3)
C(205)	5401(13)	1605(12)	−2045(9)	23(4)	C(324)	5922(14)	4182(12)	2815(10)	30(5)
O(206)	5935(9)	1356(8)	−1505(6)	26(3)	C(325)	6934(14)	4809(13)	2732(9)	31(5)

[a] Equivalent isotropic U defined as one-third of the trace of the orthogonalized U_{ij} tensor.

distances in the KSn_9^{3-} unit were found to range from 3.552(2) to 3.762(2) Å (average 3.689(4) Å), while the two longer K···Sn distances were 4.114(3) and 4.220(2) Å. As in the case of the KSn_9^{3-} structure, the final electron density difference map (maximum and minimum peaks at +2.69 and −2.99 e $Å^3$, respectively) showed no evidence of coordinated en solvent molecules about either of the uncomplexed potassium atoms.

All Pb−Pb contacts range from 3.039(1) to 3.434(2) Å (Table 2) and are shorter than the Pb−Pb distances found in lead metal (3.49 Å)[43] but are longer than the Pb−Pb bonds found in Ph_3-Pb−Pb−[C(SiMe)$_3$]Ph_2 (2.908(1) Å)[44] and Pb_2Ph_6 (2.844(4) Å).[45] The shortest Pb−Pb contacts include those from the apical Pb(1) atom to the plane defined by Pb(2,3,4,5) (average 3.067(3) Å) and those in the open square face defined by Pb(6,7,8,9) (average 3.080(3) Å). The contacts between the two square planes of the square antiprism were found to be slightly longer (average 3.104(4) Å). The longest Pb−Pb contacts occur between the lead atoms in the plane defined by Pb(2,3,4,5) (average 3.373(4) Å). These contacts are longer than the equatorial-equatorial contact distances observed in the Pb_5^{2-} anion (3.238(4) Å).[22] The shortest Pb−Pb contacts in the $K^+Pb_9^{4-}$ unit are, on average, shorter than the Pb−Pb contacts of 3.15(2) and 3.16(2) Å observed in the intermetallic NaPb phase where the lead atoms form nearly-regular Pb_4 tetrahedra.[33] Similar contact relationships have been observed in the KSn_9^{3-} unit of (2,2,2-crypt-K^+)$_3KSn_9^{3-}$ [21] and in the "free" Sn_9^{4-} anion in (2,2,2-crypt-K^+)$_4Sn_9^{4-}$.[20] The best least-squares planes through the bottom (6,7,8,9) and top (2,3,4,5) four atoms are 0.0121 and 0.0071 Å, respectively. The average angles in both squares of the antiprism are 90.0(2)° (Table 3) and are comparable to those observed in Sn_9^{4-} [90.0(2)°], KSn_9^{3-} [90.0°] and Ge_9^{4-} [90.0(4)°].

The Pb_9-moiety in the cryptated transition metal−plumbide salt (2,2,2-crypt-K^+)$_4Cr(CO)_3Pb_9^{4-}$ [38] is part of a bicapped square antiprism in which the chromium occupies the otherwise open face of the *nido*-Pb_9 cluster. The shortest Pb−Pb contacts in the $Cr(CO)_3Pb_9^{4-}$ anion were found between the apical Pb(1) atom and the lead atoms in the plane defined by Pb(2,3,4,5) (average 3.065(9) Å), which also contained the longest Pb−Pb contacts (average 3.319(8) Å), while the contacts between the

(43) Wells, A. F. *Structural Inorganic Chemistry*, 4th ed.; Oxford University Press: Oxford, England, 1975; Chapter 29, p 1013.
(44) Preut, H.; Haupt, H. J.; Huber, F. Z. *Anorg. Allg. Chem.* **1972**, *388*, 165.
(45) Mallela, S. P.; Myrczek, J.; Bernal, I.; Geanangel, R. A. *J. Chem. Soc., Dalton Trans.* **1993**, 2891.

Table 3. Selected Contacts (Å) and Angles (deg) in $K^+Pb_9^{4-}$

Contacts			
Pb(1)−Pb(2)	3.039(1)	Pb(1)−Pb(3)	3.094(2)
Pb(1)−Pb(4)	3.063(2)	Pb(1)−Pb(5)	3.071(1)
Pb(2)−Pb(3)	3.354(1)	Pb(2)−Pb(5)	3.317(2)
Pb(2)−Pb(6)	3.126(2)	Pb(2)−Pb(9)	3.098(1)
Pb(2)··K(5)	3.652(1)	Pb(3)−Pb(4)	3.389(2)
Pb(3)−Pb(6)	3.082(1)	Pb(3)−Pb(7)	3.140(1)
Pb(3)··K(5)	4.057(2)	Pb(4)−Pb(5)	3.434(2)
Pb(4)−Pb(7)	3.090(2)	Pb(4)−Pb(8)	3.143(1)
Pb(4)··K(4)	3.691(1)	Pb(5)−Pb(8)	3.077(2)
Pb(5)−Pb(9)	3.076(2)	Pb(6)−Pb(7)	3.094(2)
Pb(6)··Pb(8)	4.376(2)	Pb(6)−Pb(9)	3.073(1)
Pb(6)··K(5)	3.731(1)	Pb(7)−Pb(8)	3.103(2)
Pb(7)··Pb(9)	4.334(2)	Pb(7)··K(4)	4.173(2)
Pb(8)−Pb(9)	3.050(1)	Pb(8)··K(4)	3.498(1)
Angles			
Pb(2)−Pb(1)−Pb(3)	66.3(1)	Pb(2)−Pb(1)−Pb(4)	102.2(1)
Pb(3)−Pb(1)−Pb(4)	66.8(1)	Pb(2)−Pb(1)−Pb(5)	65.8(1)
Pb(3)−Pb(1)−Pb(5)	102.0(1)	Pb(4)−Pb(1)−Pb(5)	68.1(1)
Pb(1)−Pb(2)−Pb(3)	57.6(1)	Pb(1)−Pb(2)−Pb(5)	57.6(1)
Pb(3)−Pb(2)−Pb(5)	91.8(1)	Pb(1)−Pb(2)−Pb(6)	108.3(1)
Pb(3)−Pb(2)−Pb(6)	56.7(1)	Pb(5)−Pb(2)−Pb(6)	99.7(1)
Pb(1)−Pb(2)−Pb(9)	108.5(1)	Pb(3)−Pb(2)−Pb(9)	99.2(1)
Pb(5)−Pb(2)−Pb(9)	57.2(1)	Pb(6)−Pb(2)−Pb(9)	59.2(1)
Pb(1)−Pb(3)−Pb(2)	56.1(1)	Pb(1)−Pb(3)−Pb(4)	56.2(1)
Pb(2)−Pb(3)−Pb(4)	89.6(1)	Pb(1)−Pb(3)−Pb(6)	108.0(1)
Pb(2)−Pb(3)−Pb(6)	57.9(1)	Pb(4)−Pb(3)−Pb(6)	99.2(1)
Pb(1)−Pb(3)−Pb(7)	106.6(1)	Pb(2)−Pb(3)−Pb(7)	98.9(1)
Pb(4)−Pb(3)−Pb(7)	56.3(1)	Pb(6)−Pb(3)−Pb(7)	59.6(1)
Pb(1)−Pb(4)−Pb(3)	57.0(1)	Pb(1)−Pb(4)−Pb(5)	56.1(1)
Pb(3)−Pb(4)−Pb(5)	89.2(1)	Pb(1)−Pb(4)−Pb(7)	108.6(1)
Pb(3)−Pb(4)−Pb(7)	57.8(1)	Pb(5)−Pb(4)−Pb(7)	98.2(1)
Pb(1)−Pb(4)−Pb(8)	106.5(1)	Pb(3)−Pb(4)−Pb(8)	99.0(1)
Pb(5)−Pb(4)−Pb(8)	55.6(1)	Pb(7)−Pb(4)−Pb(8)	59.7(1)
Pb(1)−Pb(5)−Pb(2)	56.7(1)	Pb(1)−Pb(5)−Pb(4)	55.8(1)
Pb(2)−Pb(5)−Pb(4)	89.4(1)	Pb(1)−Pb(5)−Pb(8)	108.0(1)
Pb(2)−Pb(5)−Pb(8)	100.0(1)	Pb(4)−Pb(5)−Pb(8)	57.4(1)
Pb(1)−Pb(5)−Pb(9)	108.2(1)	Pb(2)−Pb(5)−Pb(9)	57.8(1)
Pb(4)−Pb(5)−Pb(9)	98.6(1)	Pb(8)−Pb(5)−Pb(9)	59.4(1)
Pb(2)−Pb(6)−Pb(3)	65.4(1)	Pb(2)−Pb(6)−Pb(7)	105.0(1)
Pb(3)−Pb(6)−Pb(7)	61.1(1)	Pb(2)−Pb(6)−Pb(9)	60.0(1)
Pb(3)−Pb(6)−Pb(9)	106.0(1)	Pb(7)−Pb(6)−Pb(9)	89.3(1)
Pb(3)−Pb(7)−Pb(4)	65.9(1)	Pb(3)−Pb(7)−Pb(6)	59.3(1)
Pb(4)−Pb(7)−Pb(6)	105.8(1)	Pb(3)−Pb(7)−Pb(8)	105.5(1)
Pb(4)−Pb(7)−Pb(8)	61.0(1)	Pb(6)−Pb(7)−Pb(8)	89.9(1)
Pb(4)−Pb(8)−Pb(5)	67.0(1)	Pb(4)−Pb(8)−Pb(7)	59.3(1)
Pb(5)−Pb(8)−Pb(7)	106.0(1)	Pb(4)−Pb(8)−Pb(9)	105.9(1)
Pb(5)−Pb(8)−Pb(9)	60.3(1)	Pb(7)−Pb(8)−Pb(9)	89.6(1)
Pb(2)−Pb(9)−Pb(5)	65.0(1)	Pb(2)−Pb(9)−Pb(6)	60.9(1)
Pb(5)−Pb(9)−Pb(6)	106.4(1)	Pb(2)−Pb(9)−Pb(8)	105.7(1)
Pb(5)−Pb(9)−Pb(8)	60.3(1)	Pb(6)−Pb(9)−Pb(8)	91.3(1)

two square planes of the square antiprism (average 3.13(1) Å) and those in the square face defined by Pb(6,7,8,9) (average 3.179(8) Å) were of intermediate lengths. It appears that coordination of the $Cr(CO)_3$ moiety to the *nido*-Pb_9^{4-} cluster is accompanied by a stretching and "opening" of the cluster, since in the $Cr(CO)_3Pb_9^{4-}$ anion, the contacts between the square planes and among the lead atoms in what was the open square plane are elongated by 0.08 and 0.05 Å, respectively. A similar stretching (0.02 Å) and opening (0.10 Å) has been noted upon insertion of the neutral $Cr(CO)_3$ fragment into the open square face of the *nido*-Sn_9^{4-} anion.[46]

A comparison of the metal−metal contacts and angles in the square faces of the square antiprism in the structures of the KSn_9^{3-} and Sn_9^{4-} anions shows that the contacts within the Sn_9-moiety are not significantly altered by interactions with the noncryptated potassium atoms. In the "free" Sn_9^{4-} cluster,[20] which is considered to be only slightly distorted from C_{4v} symmetry, the Sn−Sn contacts were found to vary from 2.943-(5) to 2.973(4) Å in the open square face and from 3.193(3) to 3.308(5) Å in the square face adjacent to the capping tin atom. The analogous contacts in the KSn_9^{3-} anion were found to vary from 2.931(3) to 2.973(2) Å and from 3.171(2) to 3.303(2) Å, respectively. Distortion of the Pb_9^{4-} anion from the ideal C_{4v} symmetry is found to be less pronounced than in the "free" Sn_9^{4-} anion (see Table 5) so that the present geometry is most probably very similar to that of a "free" Pb_9^{4-} anion.

Table 4. Important Contacts (Å) and Dihedral Angles (deg) in $K^+(2,2,2\text{-crypt-}K^+)_3Pb_9^{4-}$ (**1**) and $(2,2,2\text{-crypt-}K^+)_3Pb_9^{3-}$ (**2**)

Contacts					
height			edge		
atoms	**1**	**2**	atoms	**1**	**2**
2−3	3.354	3.634	2−5	3.316	3.224
4−5	3.434	3.408	3−4	3.389	3.171
Dihedral Angles					
atom			**1**		**2**
Trigonal Prism (opposed)					
2−5−9	3−4−7		159.2(3)		175.2(3)
Cap to Cap (vicinal)					
6−7−9	7−8−9		0.7(4)		14.2(7)
1−2−3	2−3−6		30.5(4)		21.0(4)
1−4−5	4−5−8		28.8(4)		19.3(5)
Prism End to Cap (vicinal)					
2−5−9	1−2−5		31.1(4)		38.0(5)
2−5−9	2−6−9		51.9(4)		43.0(5)
2−5−9	5−8−9		52.4(4)		43.9(4)
3−4−7	1−3−4		30.8(3)		37.8(5)
3−4−7	3−6−7		52.1(4)		42.9(5)
3−4−7	4−7−8		54.4(3)		42.2(5)

Table 5. Calculated and Experimental Pb−Pb Contacts for the Pb_9^{4-} and Pb_9^{3-} Anions[a]

	Pb_9^{4-} C_{4v} point symmetry			Pb_9^{3-} C_{2v} point symmetry		
contacts	LDFT	NLDFT	expt[b]	LDFT	NLDFT	expt[b]
Pb(1)−Pb(2,3,4,5)	2.999	3.012	3.067	2.984 2.987	2.993 2.995	3.092
Pb(2,3,4,5)−Pb(2,3,4,5)	3.124	3.137	3.374	3.045 3.148	3.054 3.161	3.255 3.403
Pb(2,3,4,5)−Pb(6,7,8,9)	3.009	3.021	3.104	2.998 3.025	3.010 3.040	3.157
Pb(6,7,8,9)−Pb(6,7,8,9)	3.036	3.049	3.080	3.008 3.025	3.026 3.032	3.081

[a] Contacts in Å. [b] Average contacts.

The Pb_9^{4-} anions and (2,2,2-crypt-K^+) cations are packed along the *a*- and *b*-axes while infinite −K(4)−(Pb_9)−K(5)− chains run along the edges of the unit cell, parallel to the *c*-axis (Figure 4a). In the analogous tin structure, similar chains were found to run diagonally across the unit cell. The −K(4)−(Pb_9)−K(5)− chains and the (2,2,2-crypt-K^+) cations are packed in layers parallel to the *c*-axis so that the chains are well sheathed by the cryptated cations, with the smallest Pb−Pb separation between chains being 9.630 Å compared with 6.468 Å between clusters within the chains. All Pb···C distances are 4.036 Å or greater (sum of the van der Waals radii for Pb[47] and CH_2[48] is 4.0 Å) so that there is little or no interaction between the lead atoms in the anion and the light atoms in the cryptand. The shortest distances between a light atom in the cryptand and the unsequestered potassium atoms are 4.793 Å for K(5)−C(118) and 4.798 for K(4)−C(225) (sum of the van der Waals radius of CH_2[48] and the ionic radius of K^+ [49] is 3.3 Å).

(46) Eichhorn, B. W.; Haushalter, R. C. *J. Am. Chem. Soc.* **1988**, *110*, 8704.

(47) Bondi, A. *J. Phys. Chem.* **1964**, *68*, 441.

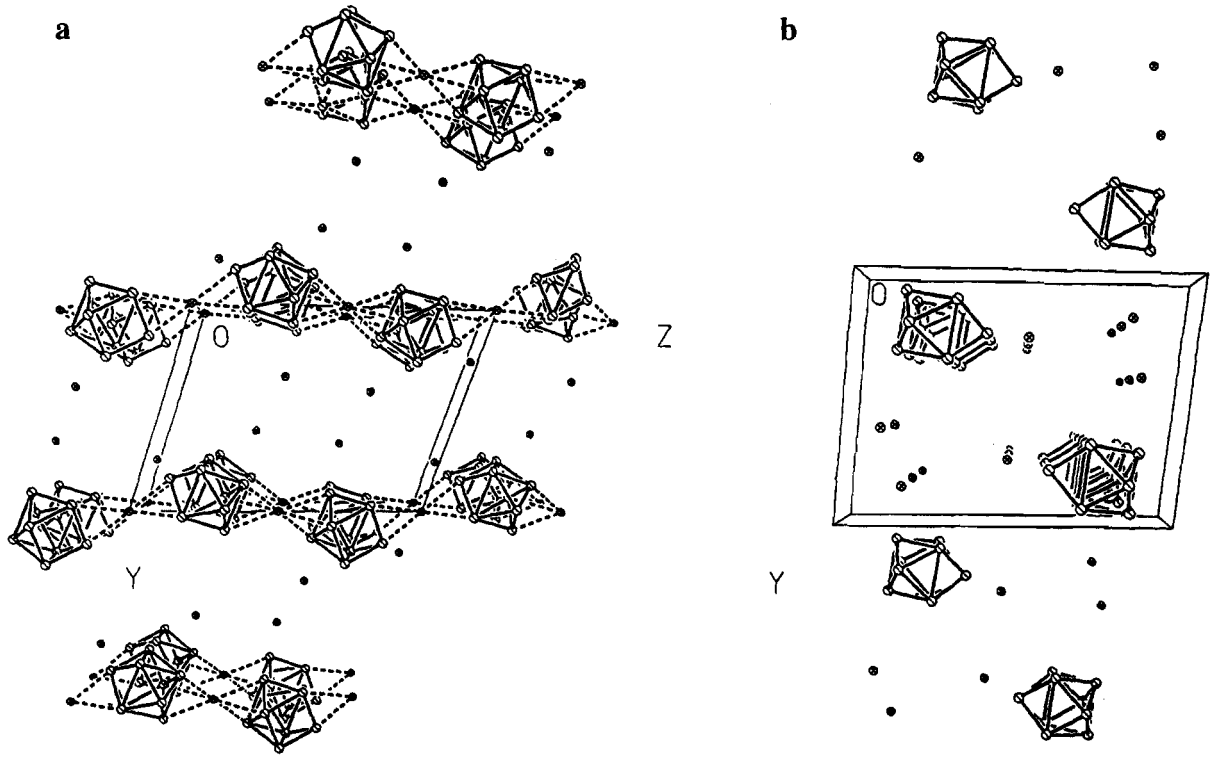

Figure 4. Unit cells of (a) $K^+(2,2,2\text{-crypt-}K^+)_3Pb_9^{4-}$ and (b) $(2,2,2\text{-crypt-}K^+)_3Pb_9^{3-}$ viewed down their *a*-axes. For clarity, only the potassium atoms in the cations have been included.

X-ray Crystal Structure of $(2,2,2\text{-crypt-}K^+)_3Pb_9^{3-}$ and Its Comparison with $(2,2,2\text{-crypt-}K^+)_3Pb_9^{3-}\cdot 0.5en$. The paramagnetic character of $(2,2,2\text{-crypt-}K^+)_3Pb_9^{3-}$ was confirmed by recording the ESR spectrum of a single crystal (orientation unknown). The spectrum was recorded at 24 °C and revealed a broad resonance at $g = 2.01$. Comparable g values were reported for the isovalent analogs Sn_9^{3-} ($g = 2.03$[19]; 2.07, 1.92[37]) and Ge_9^{3-} ($g = 1.9989$[17]; 2.04, 1.99[37]). Our value differs significantly from that of 1.68 (very broad) found by Fässler and Hunziker[37] on a powder sample. Both spectra fail to show the doublet fine structure expected for an axially symmetric species.

The crystal structure of $(2,2,2\text{-crypt-}K^+)_3Pb_9^{3-}$ consists of six cryptated potassium cations and two nine-atom lead cluster anions. The anion therefore has a charge of 3− and is consistent with an odd valence electron count for the cluster and with the paramagnetic behavior exhibited in the solid state ESR and solution NMR spectra (see **Syntheses of the Pb_9 Cluster Anions**). The most interesting feature of the structure is the Pb_9^{3-} cluster anion (Figure 2) which is in agreement with the structure recently published by Fässler and Hunziker.[37] Their values are given in square brackets and support our structural and theoretical findings, i.e., the Pb_9^{3-} anions are found to have a *closo*-C_{2v} structure similar to that observed for the Ge_9^{3-} cluster.[17,37]

The Pb−Pb contacts range from 3.050(4) to 3.634(3) [3.071(4) to 3.599(3)] Å and are comparable to those observed in the Pb_9^{4-} anion, except for the Pb(7)−Pb(9) contact which is somewhat longer (3.634(3) [3.599(3)] Å). Three groups of Pb−Pb contacts can be distinguished. The shortest Pb−Pb contacts range from 3.050(4) to 3.119(4) (average 3.09(1) [3.08(1)] Å) and are from the capping Pb(1), Pb(6), and Pb(8) atoms to the lead atoms in the trigonal prism defined by Pb(2,3,4,5,7,9) ("cap to prism" contacts). In the related Sn_9^{3-}, Ge_9^{3-} and Ge_9^{2-} anions, the "cap to prism" contacts range from 2.932(2) to 2.977(2), 2.534(4) to 2.585(4), and 2.528(6) to 2.604(5) Å, respectively. The three longest Pb−Pb distances in the Pb_9^{3-} anion range from 3.398(3) [3.395(3)] to 3.634(3) [3.599(3)] Å (average 3.480(5) [3.467(2)] Å) and correspond to the contacts between the two triangular faces defined by Pb(2,5,9) and Pb(3,4,7) of the distorted trigonal prism. Among the three longest Pb−Pb contacts, the two defining the prism height are, within experimental error (3σ), equal (3.398(4) [3.395(3)] and 3.408(4) [3.406(3)] Å). Similarly, the two contacts defining the prism height are identical in Sn_9^{3-} (3.309(2) and 3.315(2) Å) and approximately equal in Ge_9^{2-} (2.811(6) and 2.857(6) Å). In the Ge_9^{3-} anion, these contacts are not identical (3.202(4) and 3.268(4) Å) and contribute to its pronounced distortion toward C_{2v} symmetry. Interestingly, the third prism height contact in Pb_9^{3-}, corresponding to Pb(7,9), was found to be longer by ~0.23 [0.20] Å. A similar variation was also found in the Ge_9^{2-} and Ge_9^{3-} anions, where the third prism height contacts were longer and shorter by ~0.34 and ~0.41 Å, respectively. However, in the Sn_9^{3-} anion, this contact is almost equal to the other two prism height contacts and is consistent with the D_{3h} symmetry assigned to the anion. Finally, the intermediate ("prism edge") contacts in Pb_9^{3-}, which are contained in the triangular faces of the trigonal prism, range from 3.171(4) [3.165(2)] to 3.272(4) [3.259(4)] Å (average 3.224(9) [3.212(6)] Å). The contacts defining the "prism edges" are equal, within experimental error (3σ), in Sn_9^{3-} (3.058(1) and 3.060(1) Å) and Ge_9^{3-} (2.537(4) and 2.545(4) Å) and are approximately equal in Ge_9^{2-} (2.742(5) and 2.795(6) Å). When considered along with variations in specific dihedral angles (see **Comparison of the Pb_9^{4-} and Pb_9^{3-} Cluster Geometries with Structural Analogs**), the prism height ratios can be used to assess the degree of distortion (i.e., compression or elongation).

Although the packing in $(2,2,2\text{-crypt-}K^+)_3Pb_9^{3-}\cdot 0.5en$[37] is not discussed, the packing in $(2,2,2\text{-crypt-}K^+)_3Pb_9^{3-}$ exhibits several interesting features in common with its tin analogs. The Pb_9^{3-}

(48) Pauling, L. *Nature of the Chemical Bond*, 3rd ed.; Cornell University Press: Ithaca, NY, p 261.
(49) Pauling, L. *Nature of the Chemical Bond*, 3rd ed.; Cornell University Press: Ithaca, NY, p 513.

anions and (2,2,2-crypt-K^+) cations are packed along the *a*- and *b*-axes. The packing along the *c*-axis is represented in Figure 4b. The shortest anion–cation distances are in the range 3.929 [Pb(4)···C(32)] to 4.397 Å [Pb(3)···C(101)], indicating that there are no significant interactions between the lead atoms in the anion and the light atoms in the cations. The smallest Pb–Pb separations between clusters range from 8.296 to 10.247 Å. It is interesting to note that even though the unit cell of K^+(2,2,2-crypt-K^+)$_3Pb_9^{4-}$ contains two more potassium atoms than that of (2,2,2-crypt-K^+)$_3Pb_9^{3-}$, the volume of the former cell is smaller by 381 Å^3. The formation of chains in K^+(2,2,2-crypt-K^+)$_3Pb_9^{4-}$ gives rise to a more efficiently packed structure by allowing the lead clusters to be significantly closer (6.468 Å) in comparison to the shortest interanion Pb···Pb contacts in (2,2,2-crypt-K^+)$_3Pb_9^{3-}$ (8.296 Å). Analogous packing effects have been observed in the lattices of the isovalent (2,2,2-crypt-K^+)$_3KSn_9^{3-}$ and (2,2,2-crypt-K^+)$_3Sn_9^{3-}$ compounds. The volume of the former cell is smaller by 250 Å^3, and the shortest interanion Sn···Sn distances were found to be 6.675 Å in (2,2,2-crypt-K^+)$_3KSn_9^{3-}$ and 7.702 Å in (2,2,2-crypt-K^+)$_3Sn_9^{3-}$.

Computational Results. Lohr[50] has previously reported the results of relativistically corrected extended Hückel (REX) and extended Hückel (EHT) calculations on the structures of M_9^{4-} (M = Ge, Sn, Pb) clusters. The calculations showed that the *nido*-C_{4v} geometries were favored over the D_{3h} geometries as predicted by Wade's rules[51-53] and that M_9^{2-} species should favor D_{3h} geometries as exemplified by the structure of Ge_9^{2-} (the experimental geometry has approximate C_{2v} point group symmetry and can be regarded as being distorted from a D_{3h} geometry). These calculations were done with estimated, idealized geometries and without geometry optimization. Furthermore, REX and EHT calculations do not provide reliable conformational energy differences. In the present work, which now experimentally completes the series of *closo*-M_9^{3-} and *nido*-M_9^{4-} clusters of the group IV elements, we compare the optimized density functional theory (DFT) geometries of Pb_9^{3-} and Pb_9^{4-} with the experimental geometries.

The geometries of the *nido*-Pb_9^{4-} and *closo*-Pb_9^{3-} anions were calculated at the local (LDFT) and nonlocal (NLDFT) levels.[54-56] Because of the large atomic number for Pb, relativistically corrected pseudopotentials were used for the core electrons. The geometries were optimized by using analytic gradient methods and the vibrational frequencies were calculated[57] to show that the reported structures are minima on the potential energy surface. The calculated Pb–Pb contacts for Pb_9^{4-} and Pb_9^{3-} and their average experimental values are reported in Table 5. The NLDFT Pb–Pb contacts are slightly longer than those at the LDFT level. Close agreement with the experimental values is found with the largest discrepancy occurring in the Pb(2,3,4,5) plane.

The structure of the Pb_9^{4-} anion optimized to a *nido*-C_{4v} geometry. The cluster is quite fluxional as all of the calculated vibrational frequencies are in the range 100–200 cm^{-1} due to the large masses of the atoms and the long contacts between them. Second derivative analysis confirmed this symmetry[57] and showed that all vibrational frequencies are real.[58] The calculated Pb–Pb contacts in the Pb_9^{4-} anion at the LDFT and NLDFT levels are essentially the same with the contacts calculated at the NLDFT level on the order of 0.01–0.02 Å longer. A comparison of calculated Pb–Pb contacts show that the shortest Pb–Pb contacts are between the capping atom and the Pb(2,3,4,5)-plane with comparable contacts between the two planes, Pb(2,3,4,5) and Pb(6,7,8,9), forming the square antiprism, while the contacts in the open face, Pb(6,7,8,9), are 0.03 to 0.04 Å longer. The longest calculated Pb–Pb contacts are between the lead atoms in the Pb(2,3,4,5) plane, consistent with the experimental structure, and are 0.09 Å longer than the corresponding calculated Pb–Pb contacts in the open face, Pb(6,7,8,9). The calculated Pb–Pb contacts (Table 5) are shorter by 0.04 to 0.10 Å for the three shorter contacts as compared to the average experimental values with a much larger discrepancy of 0.25 Å between calculated and experimental values for the contacts in the Pb(2,3,4,5) plane. As noted above, the cluster should be quite fluxional and could easily be distorted by environmental effects in the solid state. As seen in the crystal structure, the potassium cations interact with the atoms in the Pb(2,3,4,5) plane and, coupled with the low frequencies for the cluster, there could easily be distortions of the atoms in this plane to give longer Pb–Pb contacts.

The Mulliken charge distribution in Pb_9^{4-} is essentially the same at the LDFT and NLDFT levels so only the local values are reported. The capping atom has the largest negative charge, −0.60 e, with the atoms in the open face Pb(6,7,8,9) having charges of −0.49 e. The atoms in the Pb(2,3,4,5) plane next to the capping atom have the lowest negative charge of −0.36 e.[59] If an idealized experimental geometry is used, the charges change only slightly with the charge on the capping atom changing to −0.57 e and the atoms in the adjacent plane changing by +0.01 to −0.37 e. The charges on the atoms in the open face do not change. The lowest unoccupied molecular orbital (LUMO) and second lowest unoccupied molecular orbital (SLUMO) for Pb_9^{4-} are essentially degenerate and are within 0.02 eV of each other. The highest energy molecular orbitals of the Pb_9^{4-} anion are shown in Figure 5. The highest occupied molecular orbital (HOMO) is degenerate and is predominantly localized in the open face along the Pb–Pb contacts. The second highest occupied molecular orbital (SHOMO) is not degenerate and has a large amount of electron density localized in the center of the open face with a smaller amount in the Pb(2,3,4,5) plane. The next sets of orbitals are degenerate with the higher energy one having the orbitals in the triangular faces connecting the Pb(2,3,4,5) and Pb(6,7,8,9) planes and the lower energy degenerate orbital being in the same region as well as in the triangular faces connecting the capping atom to the Pb(2,3,4,5) plane. The final two orbitals considered are very close in energy. One is essentially a lone pair on the capping atom and the other orbital is the antibonding combination of bonding sigma orbitals in the Pb(2,3,4,5) plane and presumably accounts for the longer Pb–Pb contacts in this plane.

(50) Lohr, L. L. *Inorg. Chem.* **1981**, *20*, 4229.
(51) Wade, K. *Adv. Inorg. Radiochem.* **1976**, *18*, 1.
(52) Mingos, D. M. P., *Acc. Chem. Res.* **1984**, *17*, 311.
(53) Mingos, D. M. P., *J. Chem. Soc., Chem. Commun.* **1983**, 706.
(54) Vosko, S. J.; Wilk, L.; Nusair, W. *Can. J. Phys.* **1980**, *58*, 1200.
(55) (a) Becke, A. D. *Phys. Rev. A* **1988**, *38*, 3098. (b) Becke, A. D. *The Challenge of d and f Electrons: Theory and Computation*; Salahub, D. R., Zerner, M. C., Eds.; ACS Symposium Series 394, American Chemical Society: Washington DC, 1989; pp 166. (c) Becke, A. D. *Int. J. Quantum Chem. Symp.* **1989**, *23*, 599.
(56) Perdew, J. P. *Phys. Chem. B* **1986**, *33*, 8822.
(57) Calculated vibrational frequencies (cm^{-1}): for Pb_9^{4-}, 199 (a_1), 185 (b_1), 183 (e), 173 (b_2), 168 (e), 168 (a_1), 157 (b_1), 156 (e), 152 (a_1), 144 (b_2), 141 (a_2), 133 (e), 132 (a_1), 129 (b_1), 115 (b_2); for Pb_9^{3-}, 200 (a_1), 187 (b_1), 185 (a_2), 181 (b_2), 179 (a_1), 172 (b_2), 170 (b_1), 167 (b_1), 164 (a_1), 156 (b_1), 153 (a_1), 152 (b_2), 150 (a_2), 148 (a_1), 148 (b_1), 137 (a_2), 134 (b_1), 129 (b_2), 127 (a_1), 116 (a_2), 110 (a_1).
(58) Attempts to optimize a structure beginning from D_{3h} symmetry led to a C_{2v} structure that is 13.4 kcal mol^{-1} higher in energy than the optimal C_{4v} structure at the LDFT level.
(59) The EHT and REX calculations of Lohr,[62] which did not have optimized geometries, disagree with the present calculations, i.e., the open Pb(6,7,8,9) face has the most negative charge (−0.57 and −0.54 e, respectively), the capping atom has an intermediate charge (−0.46 and −0.38 e, respectively) and the Pb(2,3,4,5) plane has the lowest negative charge (−0.31 and −0.37 e, respectively). However, our results are consistent with the CNDO results for Sn_9^{4-}:[20] Sn(6,7,8,9), −0.55 e; Sn(1), −0.75 e; Sn(2,3,4,5), −0.25 e.

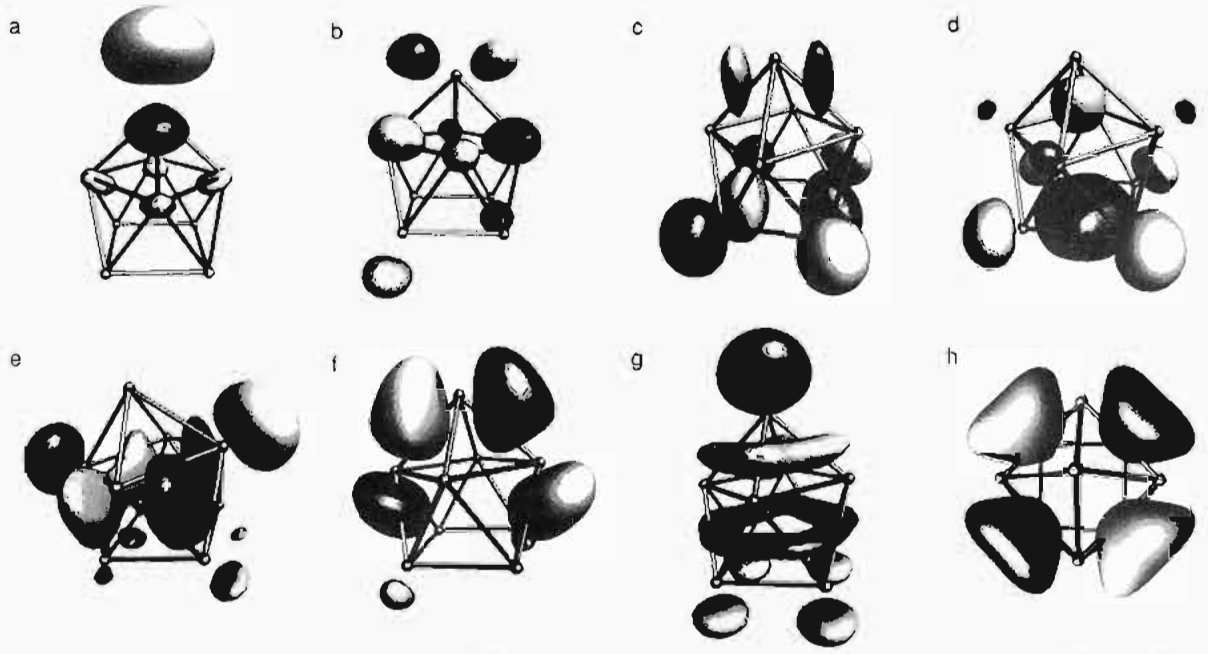

Figure 5. Molecular orbitals contoured at 0.085 for the Pb_9^{4-} anion at the LDFT level. The different shades denote the two different phases of the orbitals. Key (a) SLUMO; (b) LUMO; (c) one component of the degenerate HOMO; (d) SHOMO; one component of the degenerate (e) third and (f) fourth highest occupied MO; (g) fifth and (h) sixth highest occupied MO.

Since the HOMO of the Pb_9^{4-} anion is doubly degenerate, loss of an electron to form the Pb_9^{3-} anion lowers the symmetry from C_{4v} to C_{2v} breaking the Jahn–Teller degeneracy.[60,61] The only Pb–Pb contacts that are affected by the lowering of symmetry are those in the Pb(2,3,4,5) plane which contains two long Pb–Pb contacts of 3.148 Å and two short contacts of 3.045 Å. This result is somewhat surprising as the highest occupied molecular orbitals do not have significant components on these atoms. However, as noted above, the atoms in the Pb(2,3,4,5) plane have the longest bonds and presumably the weakest interactions and consequently would be expected to change the most on removal of an electron. This type of result is consistent with the fact that the total energy is not the sum of the orbital eigenvalues in a molecular orbital framework.

The average of the two contacts in the Pb(2,3,4,5) plane is 3.096 Å, which is only 0.03 Å shorter than the corresponding contacts in the Pb_9^{4-} anion. This shortening is consistent with the shortening of the other Pb–Pb contacts when an electron is removed from Pb_9^{4-} to form the Pb_9^{3-} anion.

The Mulliken charge distribution in Pb_9^{3-} follows the same trend that was established for the Pb_9^{4-} anion with the exception that there is less negative charge on each lead atom. In the Pb_9^{3-} anion, the capping atom has a charge of −0.42 e and charges of −0.37 and −0.36 e on the two symmetry unique atoms in the Pb(6,7,8,9) plane. The lowest negative charge of −0.28 e is found on the lead atoms in the Pb(2,3,4,5) plane. Removal of the electron from the Pb_9^{4-} anion, which reduces the symmetry to C_{2v} point symmetry, leads to a rotation of the SOMO orbitals by 45° (as compared to the HOMO of Pb_9^{4-}) so that this orbital now bisects the Pb–Pb contacts. This manifests itself in the spin density, shown in Figure 6, which basically follows the form of the SOMO.

The bonding in Pb_9^{3-} and Pb_9^{4-} involves only s- and p-orbitals and the valence s-orbitals are fully occupied. There

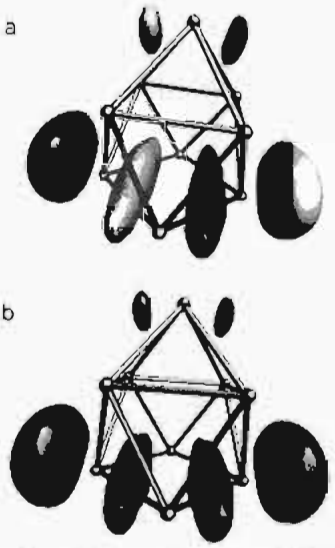

Figure 6. (a) Singly occupied molecular orbital (SOMO) and (b) spin density at 0.008 e/Å^3 for the Pb_9^{3-} anion at the LDFT level. The different shades denote the two different phases of the orbitals.

is no d-orbital population even though valence d-orbitals were included in the calculations. The "s"-orbitals are essentially doubly occupied and each "p"-orbital has the remainder of the electron population.

Comparison of the Pb_9^{4-} and Pb_9^{3-} Cluster Geometries with Structural Analogs. The computational findings indicate that the *nido*-C_{4v} geometry of Pb_9^{4-} and the *closo*-C_{2v} geometry of Pb_9^{3-} are true minima, and the flexibility of both clusters is implied by the low values of their calculated vibrational frequencies. Previous studies have shown that selected M–M contacts and dihedral angles in nine-atom clusters can provide a quantitative assessment of their geometries in terms of distortions from ideal C_{4v} and D_{3h} symmetries. Angles defining the degree of "squareness" of the base in a C_{4v} structure, the dihedral angles between selected faces of the polyhedron[31,62]

(60) Attempts to optimize a structure beginning from D_{3h} symmetry led to a C_{2v} structure that is 7.5 kcal mol^{-1} higher in energy that the optimal C_{2v} structure at the LDFT level.

(61) (a) Jahn, H. A.; Teller, E. *Proc. R. Soc. London* **1937**, *161A*, 220 (b) Herzberg, G. *Molecular Spectra and Molecular Structure, III. Electronic Spectra and Electronic Structure of Polyatomic Molecules*, Van Nostrand Reinhold: NewYork, 1966; pp 37–68.

(62) Guggenberger, L. J.; Muetterties, E. L. *J. Am. Chem. Soc.* **1974**, *96*, 1748.

Table 6. Selected Dihedral Angles in Nine-Atom Polyhedra[a]

					dihedral angles (deg)										
						cap to cap (vicinal)				prism end to cap (vicinal)					
cluster	space group	pt sym	no. of skeletal e⁻	*h*:*e* ratio	trigonal prism (opposed)	base	cap to antiprism			vicinal, waist					ref
Bi_9^{5+}	$P6_3/m$	D_{3h}	22	1.15	180	22	22	22		43	43	43	43	43	48
Sn_9^{3-}	$P\bar{1}$	D_{3h}	21	1.08	179	17	18	18		40	40	41	41	41	42	19
Bi_9^{5+}	Pnnm	C_{2v}	22	1.14	174	14	24	24		41	43	48	48	48	48	50
Pb_9^{3-}	$P\bar{1}$	C_{2v}	21	1.05	175	14	19	21		38	38	42	43	43	44	*b*
Ge_9^{3-}	$P\bar{1}$	C_{2v}	21	1.27	170	32	14	17		50	51	41	42	43	43	17
Ge_9^{2-}	$P\bar{1}$	C_{2v}	20	1.01	171	8	23	25		36	38	44	45	45	47	16
Ge_9^{4-}	$P\bar{1}$	$\sim C_{4v}$	22	1.05	162	5	24	32		32	33	51	51	53	54	16
Sn_9^{4-}	$P\bar{1}$	C_{4v}	22	1.02	158	3	29	30		29	32	52	53	54	55	20
KSn_9^{3-}	$P\bar{1}$	C_{4v}	22	1.02	160	2	28	29		31	31	51	52	54	54	21
$K^+Pb_9^{4-}$	$P\bar{1}$	C_{4v}	22	1.01	159	1	29	31		31	31	52	52	52	54	*b*

[a] Dihedral angles were calculated from original structural data. The uncertainties in the dihedral angles were calculated using the uncertainties in the atomic coordinates and range from 0.3 to 0.8°. [b] Present work.

and the height to edge (*h*:*e*) ratios must be considered.[63,64] Major changes in selected dihedral angles involving the two lead clusters and their comparison with those of other known nine-atom polyhedra are given in Table 6 following the method outlined previously.[16,20]

A nine-atom cluster having an ideal tricapped trigonal prismatic geometry (D_{3h} point symmetry) must possess a 3-fold axis passing through the trigonal faces of the prisms defined by atoms 2−5−9 and 3−4−7. The dihedral angle between these two faces, referred to as the "trigonal prism" (opposed) dihedral angle, must be 180°, and the bond lengths between the atoms in the triangular faces must be equivalent. The dihedral angles between faces 1−2−3, 2−3−6; 1−4−5, 4−5−8; and 6−7−9, 7−8−9, which are joined by a common prism height parameter 2−3, 4−5, or 7−9, are referred to as "cap to cap" (vicinal) dihedral angles and must be equivalent. Moreover, the dihedral angles between the trigonal prismatic face (e.g., 2−5−9) and the three adjoining faces (e.g., 1−2−5, 2−6−9, and 5−8−9) are referred to as "prism end to cap" (vicinal) dihedral angles and must also be equivalent. These requirements must be met to allow for a 3-fold rotation into an indistinguishable conformation. There are no requirements for the *h*:*e* ratio.

For the ideal monocapped square antiprismatic geometry (C_{4v} point symmetry), the nine-atom cluster must possess a 4-fold axis passing through the center of the square antiprism and the apical atom. This requires the open square face, defined by atoms 6, 7, 8, and 9, to be planar (i.e., the dihedral angle between faces 6−7−9 and 7−8−9 of the open square face must be zero) and the diagonals of this face to be equivalent. Two of the "cap to cap" (vicinal) dihedral angles (1−2−3, 2−3−6 and 1−4−5, 4−5−8) must equal two of the "prism end to cap" (vicinal) dihedral angles (Tables 4 and 6) and consist of dihedral angles between one face of the trigonal prism and a face containing a capping atom (referred to as "cap to antiprism" angles). The dihedral angles about the waist of the square antiprism (referred to as the "vicinal, waist" angles) must also be equivalent. Two other dihedral angles used to assess C_{4v} symmetry are defined by the two pairs of opposing triangular faces having one atom on the square base. One pair of triangular faces 2−5−9 and 3−4−7 defines the dihedral angle referred to as the "trigonal prism" (opposed) and is also used to assess D_{3h} symmetry (Table 6). The second pair of triangular faces defines the dihedral angle referred to as the "alternate prism" (opposed). For a structure possessing C_{4v} symmetry, these two dihedral angles must be equivalent. Also, the *h*:*e* ratio must be unity to obtain ideal square faces within the square antiprism. These requirements must be met to allow for a 4-fold rotation to an indistinguishable mapping of atoms.

An irregular tricapped trigonal prismatic geometry of C_{2v} symmetry has angle relationships similar to those of the C_{4v} case. However, the C_{2v} structure neither requires an open square face nor does the "cap to cap (vicinal)" dihedral angle between faces 6−7−9 and 7−8−9 have to be equal to zero. As for the D_{3h} case, there is no restriction on the *h*:*e* ratio.

An examination of specific dihedral angles and the *h*:*e* ratio in Pb_9^{4-} (Table 6) reveals that all the requirements for C_{4v} symmetry are met, i.e., the *h*:*e* ratio is 1.01, the dihedral angle between the two triangular faces defined by atoms 6−7−9 and 7−8−9 is 1° instead of 0° (the mean deviation from the plane is only 0.0071 Å) and the "cap to prism" (vicinal) dihedral angles are equal within experimental error ($\pm 3\sigma$). The "trigonal" and "alternate prism" dihedral angles were found to be almost equivalent (159 and 157°) for the *nido*-Pb_9^{4-} anion and are also in accord with C_{4v} symmetry. The dihedral angles and *h*:*e* ratios (Table 6) indicate that the Pb_9^{4-} anion is isosteric with the Sn_9^{4-} anion in both $(2,2,2\text{-crypt-}K^+)_4Sn_9^{4-}$ [20] and $(2,2,2\text{-crypt-}K^+)_3KSn_9^{3-}$.[21] Within each category of dihedral angles, the values of the angles are essentially identical for the three isovalent species. It is also interesting to note that the differences in the dihedral angles in both structures of the Sn_9^{4-} anion are not significant and follow the trend found for the contacts and bond angles in Pb_9^{4-}, confirming that, upon bridging with the alkali metal counterion, the C_{4v} symmetry of the anions is retained. The only noticeable difference was found between the "trigonal prism" (160°) and "alternate prism" (156°) dihedral angles in KSn_9^{3-}; these angles are identical in the "free" Sn_9^{4-} anion, i.e., 158° and intermediate when compared to values found in KSn_9^{3-}. The Ge_9^{4-} anion, despite its low *h*:*e* ratio (1.05), is significantly distorted towards C_{2v} symmetry. The square base deviates from planarity by 5°, and the "trigonal prism" dihedral angle (162°) is larger than the "alternate prism" dihedral angle (156°). Moreover, one of the "cap to antiprism" dihedral angles (24°) is found to be significantly smaller than the remaining three (32, 33, and 33°). It is concluded that the Pb_9^{4-} anion in $K^+(2,2,2\text{-crypt-}K^+)_3Pb_9^{4-}$ possesses a monocapped square antiprismatic geometry and agrees with the present calculated geometry and that predicted by Wade's rules (*vide infra*).

The experimentally determined geometry of the *closo*-Pb_9^{3-} anion can be described as a distorted C_{4v} structure. Unambiguous classification of the symmetry of Pb_9^{3-} is not as straightforward as for the *nido*-Pb_9^{4-} anion. The most significant differences between the possible D_{3h} and C_{2v} symmetries are in the "cap to cap" (vicinal) and "trigonal prism" (opposed) dihedral angles. The D_{3h} symmetry requires the first set of

(63) Porai-Koshits, M. A.; Aslanov, L. A. *Zh. Strukt. Khim.* **1972**, *13*, 266.
(64) O'Neill, M. E.; Wade, K. *Polyhedron* **1983**, *2*, 963.

angles to be equivalent and the second set to be 180°. In contrast, C_{2v} symmetry only requires two of the "cap to cap (vicinal)" dihedral angles to be equal. The requirements for D_{3h} symmetry are met in the Sn_9^{3-} anion (17, 18, 18 and 179°) but not for the isovalent Pb_9^{3-} (14, 19, 21 and 175°) and Ge_9^{3-} (32, 14, 17 and 170°) anions, where distortions from D_{3h} symmetry are significantly more pronounced. The magnitudes of the different classes of dihedral angles and *h*:*e* ratios (Table 6) indicate that the Pb_9^{3-} anion is only isostructural with the Ge_9^{2-} anion. In particular, the "cap to cap" (vicinal) and "prism end to cap" (vicinal) dihedral angle categories in both anions contain two distinct sets of characteristic angles of equivalent magnitudes and the Pb_9^{3-} anion has an *h*:*e* ratio close to unity (1.05). The experimentally determined geometry of the *closo*-Pb_9^{3-} cluster anion therefore should be considered to have C_{2v} point symmetry, in agreement with the theoretical findings which show that the geometry of Pb_9^{3-} derives from C_{4v} symmetry (*vide infra*).

The structures of M_9^{m-} (M = Ge, Sn, and Pb; $m = 2$ or 4) can be predicted by Wade's rules as they possess $2n + 2$ skeletal electrons for $m = 2$ and $2n + 4$ skeletal electrons for $m = 4$ if only the valence p-orbitals are considered.[51-53] This is a good approximation for the Pb clusters as the calculations show the valence s-orbitals to be fully occupied. The structures of the M_9^{4-} are predicted to be monocapped square antiprisms of approximate C_{4v} point symmetry and are derived from *nido*-10-vertex polyhedra. The experimental structures of the *nido*-Pb_9^{4-} and *nido*-Sn_9^{4-} anions are consistent with Wade's rules whereas that of the *nido*-Ge_9^{4-} anion is distorted towards C_{2v} point symmetry. The structures of M_9^{2-} clusters, which can be considered as two electron oxidation products of *nido*-M_9^{4-} clusters, are predicted by Wade's rules to be *closo*-nine-vertex polyhedra having tricapped trigonal prismatic geometries of approximate D_{3h} point symmetry. The only known example of a M_9^{2-} cluster is the Ge_9^{2-} anion whose structure is distorted from the ideal D_{3h} point symmetry as predicted by Wade's rules. Oxidative *nido*−*closo* cluster closing normally occurs on removal of an electron pair. The degeneracies of M_9^{4-} frontier orbitals cause the products resulting from the removal of a single electron to be clusters having an incompletely filled molecular orbital which relieves the degeneracy by means of a Jahn−Teller distortion.[61,65] Consequently, the geometries of the paramagnetic M_9^{3-} clusters are also regarded as *closo*-structures derived from C_{4v} symmetry, but are Jahn−Teller distorted to C_{2v} symmetry. While the structure of the *closo*-Sn_9^{3-} anion is most akin to a tricapped trigonal prism of D_{3h} point symmetry, those of the *closo*-Ge_9^{3-} and *closo*-Pb_9^{3-} anions derive from monocapped square antiprismatic (C_{4v}) geometries that have been distorted to C_{2v} symmetry.

The *h*:*e* ratio has been shown to correlate with the electron count for *closo*-D_{3h} nine-atom clusters.[63,64] If one counts only the valence p-electrons (2n) and the additional charges, −2, −3, or −4 then one has 10 or 11 occupied orbitals containing the p-atomic orbitals for a nine atom group IV cluster having a charge between −2 and −4. For tricapped trigonal prismatic nine-atom homonuclear clusters, Wade suggests that the two highest 10th and 11th molecular orbitals (the HOMO and LUMO of the dianion, respectively) are nondegenerate and can, in principle, gain one or two electrons without a change in symmetry from that of the *closo*-cluster with $(n + 1)$ electron pairs. In Wade's qualitative model, the frontier molecular orbitals of *closo*-M_9^{2-} clusters (M = Ge, Sn and Pb) consist of HOMO orbitals having a_2' symmetry which are predominantly bonding in character and LUMO orbitals having a_2'' symmetry which are predominantly antibonding in character. The combination of atomic p-orbitals that contribute to the HOMO molecular orbitals are bonding for the M−M contacts referred to as "height" and antibonding for the "edge" M−M contacts while the LUMO orbitals are precisely the reverse: bonding for "edge" M−M contacts and antibonding for "height" M−M contacts. The *closo*-Ge_9^{2-} cluster (C_{2v} point symmetry), the only group IV example of a *closo*-cluster having 20 skeletal electrons, has a *h*:*e* ratio equal to 1.01. The addition of an electron to the *closo*-M_9^{2-} cluster to generate *closo*-M_9^{3-} is expected to bring about shortening of the "edge" and lengthening of the "height" M−M contacts as a result of filling the antibonding LUMO molecular orbital of the M_9^{2-} cluster. Consequently, a higher value for the *h*:*e* ratio is expected for the *closo*-M_9^{3-} clusters having 21 skeletal electrons than for the *closo*-M_9^{2-} cluster having 20 skeletal electrons as exhibited by the *closo*-Pb_9^{3-} (C_{2v}), *closo*-Sn_9^{3-} (D_{3h}) and *closo*-Ge_9^{3-} (C_{2v}) clusters which have higher *h*:*e* ratios of 1.05, 1.08, and 1.27, respectively. Optimization of the Pb_9^{2-} cluster at the LDFT level starting from a structure with D_{3h} symmetry led to a structure with C_{2v} symmetry.[66] The resulting C_{2v} symmetry structure can be regarded as being derived from a D_{3h} structure based on the charge distribution. The charge distribution shows that there are three approximately equivalent atoms which correspond to the original plane of atoms that were not contacting each other and six equivalent atoms corresponding to those from the upper and lower trigonal faces. The C_{2v} distortion makes one of the three noncontacting equivalent atoms a cap atom as in the C_{4v} structure. However, rather than having an open face in the basal plane of four atoms in a C_{4v} structure, two of the atoms remain in contact with each other. Thus, the difference between the D_{3h} and C_{4v} structures revolves mostly about whether a short contact between two atoms is present in the "open" basal face or not.

The *closo*-Pb_9^{3-} anion, with one less electron than the *nido*-Pb_9^{4-} anion, is better viewed as a rearrangement from *nido*-C_{4v} to *closo*-C_{2v} symmetry involving simultaneous compressions and elongations of Pb−Pb contacts in the *nido*-Pb_9^{4-} anion. The Pb(1) atom, which caps the four Pb(2,3,4,5) atoms defining the height of the trigonal prism (i.e., 2−3 and 4−5), remains a capping atom while Pb(6) and Pb(8) become capping atoms by undergoing an elongation of ~0.603 Å with simultaneous compressions of the Pb(7)−Pb(9) distance and the edges of the C_{4v} structure, Pb(2)−Pb(5) and Pb(3)−Pb(4), by ~0.742 and ~0.14 Å, respectively. The rearrangement is such that the four lead atoms Pb(6,7,8,9) are no longer coplanar, thereby destroying the 4-fold symmetry axis through Pb(1). The resulting C_{2v} structure can be regarded as a distorted tricapped trigonal prism having experimental prism heights defined by Pb(2)−Pb(3), 3.398(3) Å; Pb(4)−Pb(5), 3.408(3) Å; and Pb(7)−Pb(9), 3.634-(3) Å. The Pb(7)−Pb(9) distance is the longest contact among the three prism heights and determines if the structure is *closo* or *nido*. In principle, the Pb_9^{3-} structure is intermediate but most akin to a *closo* structure since the distance is only 0.22 Å longer that the other prism heights and 0.74 Å shorter that the diagonal distances of the basal plane of *nido*-Pb_9^{4-}. Thus, the C_{2v} structure of Pb_9^{3-} lies between the *nido*-C_{4v} and *closo*-D_{3h} limits for M_9 species. The conversion between the *nido*-C_{4v} and *closo*-D_{3h} structures for M_9 species is energetically possible, since theoretical calculations suggest that the energy barrier to conversion is less than 0.1% of the total orbital energy of either symmetry and can be assumed likely to occur in solution.[31] Moreover, the low energy barrier to C_{4v}−D_{3h} interconversion and the calculated low vibrational frequencies of the Pb_9 clusters

(65) O'Neill, M. E.; Wade, K. *J. Mol. Struct.* **1983**, *103*, 259.

(66) Campbell, J.; Dixon, D. A.; Mercier, H. P. A.; Schrobilgen, G. J. *J. Am. Chem. Soc.*, to be submitted for publication.

suggest that crystal lattice effects may play a role in establishing the geometries of the M_9 clusters in the solid state.

Conclusions

The Pb_9^{4-} anion has eluded isolation and definitive structural characterization since its solutions were first prepared over 100 years ago by Joannis,[4,5] despite its correct formulation by Kraus[8] and Zintl.[10] The *nido*-Pb_9^{4-} and *closo*-Pb_9^{3-} anions complete the series of group IV M_9^{4-} and M_9^{3-} (M = Ge, Sn, Pb) naked cluster anions that have been structurally characterized by X-ray crystallography. The *nido*-Pb_9^{4-} anion is, after its isovalent KSn_9^{3-} anion, the second example of a nine-atom polyhedron bridged to two non-cryptated potassium cations. The Pb_9^{4-} cluster preserves its monocapped square antiprismatic geometry upon bridging to free potassium cations, and reveals a symmetry, among the *nido*-M_9^{4-} clusters, that is closest to the ideal C_{4v} symmetry predicted by Wade's rules. The Pb_9^{3-} anion is a rare example of a paramagnetic cluster and is only the third example of a paramagnetic nine-atom polyhedron. Among the *closo*-nine-atom clusters, the *h*:*e* ratio for the *closo*-Pb_9^{3-} anion is of an intermediate value and consequently follows the correlation between *h*:*e* ratio and electron count noted by Wade. Theoretical calculations at the LDFT and NLDFT levels indicate that the experimentally observed C_{4v} geometry of *nido*-Pb_9^{4-} and C_{2v} (distorted from C_{4v}) geometry of *closo*-Pb_9^{3-} are the true minima. Loss of an electron from the degenerate HOMO of Pb_9^{4-} to form Pb_9^{3-} breaks the Jahn–Teller degeneracy, lowering the anion symmetry from C_{4v} to C_{2v}.

Experimental Section

Apparatus and Materials. All compounds used and prepared during the course of this work were air- and moisture-sensitive. Consequently, all manipulations were carried out under anhydrous and oxygen-free conditions on a glass vacuum line, equipped with glass/Teflon grease-free stopcocks (J. Young Scientific Glassware), and in a two-station nitrogen-atmosphere drybox (Vacuum Atmospheres Model DLX). Drybox moisture and oxygen levels were <0.1 ppm.

The oxide layer on large pieces of potassium metal (MCB, >99%), stored under paraffin oil, was cut off and the paraffin oil removed by washing the freshly-cut samples with petroleum ether (Fisher, boiling range 60–80 °C). The metal pieces were immediately transferred into a dry tube and the residual ether removed under vacuum before the clean metal was transferred into the drybox. Prior to alloy preparation, the potassium metal was recut in the drybox to give clean metal surfaces. Lead metal as shot (BDH, 99.9%) and 2,2,2-crypt (4,7,13,16,21,24-hexaoxa-1,10-diazabicyclo [8.8.8]hexacosane; Merck, 99%) were dried in the evacuated port of the drybox for at least 45 min followed by exposure to the atmosphere of the drybox for at least 2 days prior to use. Ethylenediamine (Fisher, 99%) was initially dried over CaH_2 (MCB) for several weeks and then vacuum distilled onto and stored over fresh CaH_2 for at least an additional week prior to use. Tetrahydrofuran (Fisher, 99.9%) was dried over sodium wire for several weeks prior to use.

Preparation of $KPb_{2.05}$ Alloy. The alloy was prepared by fusing potassium (0.5217 g, 13.34 mmol) and lead (5.6687 g, 27.36 mmol) in the molar ratio 1:2.05 in a dry thick-walled Pyrex tube in the flame of a Meeker burner, until completely molten. After complete reaction, the alloy was allowed to cool and solidify, and it was transferred to the drybox where it was ground to a fine powder and stored in a glass vial until used.

Extraction of the Alloy Phase. Stoichiometric amounts of 2,2,2-crypt, corresponding to potassium in the metal alloy, were transferred into either a precision thin-walled 10-mm o.d. Pyrex NMR tube (Wilmad) or into a Pyrex ampule (used in the second step for crystal growing) that had been glassblown onto a Pyrex reaction vessel (used in the first step for the extraction of the alloy). The powdered alloy was then transferred into the reaction vessel. The two reactants were initially kept separate in order to prevent possible oxidation of the alloy by 2,2,2-crypt. After evacuation, en was vacuum distilled onto the alloy: ca. 10 mL for NMR samples and ca. 5 mL for crystal growing. Extraction of the alloy commenced as soon as the mixture had warmed to room temperature and was indicated by the intense brown colors of the solutions. The solutions are extremely air sensitive, so that any leaks in the system resulted in immediate decomposition of the solutions as evidenced by concomitant loss of color and plating out of a lead mirror on the walls of the reaction vessel. The 2,2,2-crypt was added to the brown en solution the day following commencement of extraction. Upon addition of an excess of 2,2,2-crypt with respect to potassium in the alloy, the solution immediately turned deep emerald green. In contrast, the use of excess alloy with respect to 2,2,2-crypt resulted in a dark brown solution having a green tint. The samples were generally extracted for approximately 1 week following addition of 2,2,2-crypt and were periodically agitated during the extraction period.

Preparation and Isolation of $K^+(2,2,2\text{-crypt-}K^+)_3Pb_9^{4-}$ and $(2,2,2\text{-crypt-}K^+)_3Pb_9^{3-}$. Following extraction of $KPb_{2.05}$ (0.1585 g, 0.3417 mmol) in en, thin dark red needle-shaped crystals appeared several hours after addition of 50% of the stoichiometric amount of 2,2,2-crypt (0.0646 g, 0.1716 mmol) to the dark brown solution. The brittle dark red needles failed to diffract, but as noted above, their morphology resembled that of $(2,2,2\text{-crypt-}Na^+)_2Pb_5^{2-}$.[20] The use of a small stoichiometric excess of 2,2,2-crypt (0.117 g, 0.2967 mmol) with respect to the alloy (0.1066 g, 0.2298 mmol) resulted in an intense emerald green solution. Generally, after 1 week of extraction of the alloy in en, an excess of THF (1.5:1 v:v) was statically distilled into the vessel at 0 °C. The reactors were allowed to stand so that THF slowly vapor phase diffused into the en solutions. Vapor diffusion of THF into the dark brown and emerald green solutions led to the formation of large dark red hexagonal crystals of $K^+(2,2,2\text{-crypt-}K^+)_3Pb_9^{4-}$ and large dark red parallelepiped crystals of $(2,2,2\text{-crypt-}K^+)_3Pb_9^{3-}$, respectively. After several weeks, the emerald green solution obtained from the extraction of $KPb_{2.05}$ with a stoichiometric excess of 2,2,2-crypt returned to its original dark brown color. Addition of THF to this dark brown solution led to the formation of long thin dark red needle-like crystals, whose morphology resembled that of the crystals of $(2,2,2\text{-crypt-}Na^+)_2Pb_5^{2-}$ and also failed to diffract. The mother liquors were decanted into the attached Pyrex vessels and slowly pumped off under dynamic vacuum. Once all the solvent has been removed, the crystals were dried under dynamic vacuum. The dry samples were transferred to a drybox equipped with a microscope and the reaction vessels cut open. Several crystals were mounted in 0.4–0.5 mm Lindemann glass capillaries which were stored at room temperature prior to mounting on the diffractometer. The crystals used for X-ray crystal structure determination had the following dimensions: 0.4 × 0.5 × 0.6 mm ($K^+(2,2,2\text{-crypt-}K^+)_3Pb_9^{4-}$), and 0.4 × 0.4 × 0.6 mm ($(2,2,2\text{-crypt-}K^+)_3Pb_9^{3-}$).

Electron Spin Resonance Spectroscopy. A large parallelepiped-shaped crystal of $(2,2,2\text{-crypt-}K^+)_3Pb_9^{3-}$ was transferred inside the drybox into a 3-mm o.d. quartz tube which had been previously dried and flamed out under vacuum. The tube was then evacuated and flame sealed. Prior to the experiment, the ESR spectrum of the empty quartz tube had been recorded in order to check for the presence of paramagnetic contaminants.

The ESR spectra were recorded at room temperature on a Bruker ER 100 D spectrometer operating at a frequency of 9.445 GHz (X-band) with a magnetic field modulation of 100 kHz, a modulation amplitude of 10 G, and a microwave power of 15 dB.

^{207}Pb NMR Spectroscopy. Following extraction of the alloys in en, any undissolved material was allowed to settle before the solutions were decanted into precision 10-mm o.d. Pyrex NMR tubes (Wilmad). The solutions were then concentrated by static distillation of en from the NMR tubes by cooling the portion of the vessel containing the residual alloy in an ice-water bath. Once the solutions were sufficiently concentrated for NMR analysis (i.e., 4 to 5 cm of solution remaining in each NMR tube), the NMR tubes and contents were isolated by flame sealing.

The ^{207}Pb NMR spectra were recorded on a Bruker AM-500 pulse spectrometer at 30 °C. Spectra were obtained without locking (field drift < 0.1 Hz h^{-1}) using a 10-mm probe broad banded over the frequency range of 23–202 MHz (11.475 T). The operating frequency for ^{207}Pb was 104.631 MHz. A pulse width of 25 μs, corresponding to a bulk magnetization tip angle of approximately 90°, was used. Free induction decays were typically accumulated in a 16 K memory. A spectral width setting of 50 kHz was employed, yielding a data point

resolution of 6.1 Hz and acquisition time of 0.328 s. Samples typically required the acquisition of 5000−10000 transients per spectral scan range.

The ^{207}Pb spectra were referenced to a neat sample of $(CH_3)_4Pb$ at 30 °C. The chemical shift convention used was a positive (negative) shift signifies a chemical shift to high (low) frequency of the reference compound.

Crystal Structure Determination of K^+(2,2,2-crypt-K^+)$_3Pb_9^{4-}$ and (2,2,2-crypt-K^+)$_3Pb_9^{3-}$. The experimental values for (2,2,2-crypt-K^+)$_3Pb_9^{3-}$ are reported as Supporting Information, along with details on the refinement of the structure.

Collection and Reduction of X-ray Data. Crystals of K^+(2,2,2-crypt-K^+)$_3Pb_9^{4-}$ were centered on a Syntex P3 diffractometer, using silver radiation monochromatized with a graphite crystal (λ = 0.560 86 Å). Accurate cell dimensions were determined at $T = -100$ °C from least-squares refinement of the setting angles (χ, φ, and 2θ) obtained from 44 centered reflections (with $11.0° \leq 2\theta \leq 28.7°$) chosen from a variety of points in reciprocal space. Integrated diffraction intensities were collected using an ω-scan technique with scan rates varying from 1.5 to 14.6°/min in ω and a scan range of ± 0.5° so that the weaker reflections were examined more slowly to minimize counting errors. Data were collected with $0 \leq h \leq 22$, $-22 \leq k \leq 21$ and $-30 \leq l \leq 30$ and with $3° \leq 2\theta \leq 47°$. During data collection, the intensities of three standard reflections were monitored every 97 reflections to check for crystal stability and alignment. A total of 28 390 reflections were collected out of which 871 were standard reflections. The intensities of the standards dropped regularly to about 75% of their original values during the course of the data collection; intensity decay arising from crystal deterioration was later corrected by linearly scaling the data between each set of standards. A total of 26 339 unique reflections remained after averaging of equivalent reflections. A total of 11 833 reflections, satisfying the condition $I \geq 2\sigma(I)$, were used for structure solution and refinement. Corrections were made for Lorentz and polarization effects, while absorption corrections were applied using the program DIFABS.[67]

Crystal Data. K^+(2,2,2-crypt-K^+)$_3Pb_9^{4-}$: $C_{54}H_{108}K_4N_6O_{18}Pb_9$ (fw = 3150.57), crystallizes in the triclinic system, space group $P\bar{1}$, with a = 15.811(5) Å, b = 16.173(5) Å, c = 20.180(6) Å, α = 98.60(3)°, β = 104.59(2)°, γ = 118.32(2)°; V = 4171(2) Å^3 and D_{calc} = 2.426 g cm^{-3} for Z = 2. Ag Kα radiation (λ = 0.56086 Å, μ(AgKα) = 100.3 cm^{-1}) was used.

Solution and Refinement of the Structure. Since the volume of the present cell was comparable to the one previously found for (2,2,2-crypt-K^+)$_4Sn_9^{4-}$ [20] and since the Pb_9^{4-} anion had been found in the mother liquor, the first model used in the refinement of the two structures involved eight (2,2,2-crypt-K^+) cations and two Pb_9^{4-} anions. The program XPREP[68] was used for determining the correct cells and space groups. It first confirmed the original cell and that the lattice was triclinic primitive (R_{int} = 0.112). Examination of the E-statistics (calculated, 0.902; theoretical, 0.968), showed that the structure was centrosymmetric. Consequently, the structure was solved in the $P\bar{1}$ space group.

The first solution was obtained without absorption corrections using direct methods and located the positions of the lead atoms on general positions. As expected, this solution indicated a nine-atom polyhedron, similar to that of Sn_9^{4-}.[20] The full-matrix least-squares refinement of the lead atom positions and isotropic thermal parameters gave a conventional $R = (\Sigma||F_o| - |F_c||/\Sigma|F_o|)$ of 0.213. At this point, the positions of the three potassium atoms in the three 2,2,2-crypt-K^+ cations were readily deduced on general positions as well as two more large peaks at the centers of symmetry 0,0,0 and 0,0,$^1/_2$ for two other potassium atoms which, as in the (2,2,2-crypt-K^+)$_3KSn_9^{3-}$ structure,[21] bridge two polyhedra. Successive difference Fourier syntheses revealed the general positions of the remaining nitrogen, oxygen and carbon atoms. Significant improvement of the structure was achieved by introducing the positions and isotropic thermal parameters for all the N, O, and C atoms as well as the calculated values of the positions of the hydrogen atoms [d(C−H) = 0.96 Å; U(H) fixed to 0.08 Å^2]; the R-factor dropped to R = 0.106. In order to reduce the computation time, refinement of the full structure was successively cycled among the heavy atom anions, including the two bridging potassiums for K^+(2,2,2-crypt-K^+)$_3Pb_9^{4-}$, and each of the three 2,2,2-crypt-K^+ cations. The lead and potassium atoms were ultimately refined with anisotropic thermal parameters, while the light atoms in the ligands were restricted to isotropic thermal parameters, producing another improvement in the structure solution (R = 0.080).

The structure was solved a second time using data that had been corrected for absorption. The solution obtained (R = 0.091) indicated a slight improvement over that obtained without absorption corrections (R = 0.106). The final refinement was obtained by introducing anisotropic thermal parameters for the Pb and K atoms (R = 0.069) and setting the weight factor $w = 1/[\sigma^2(F) + 0.000005F^2]$, which gave rise to the final residual, R, of 0.0673 (R_w = 0.0447). In the final difference Fourier maps, the maximum and minimum electron densities were +2.69 and −2.99 eÅ^{-3}. The residual electron density was mainly located around the Pb_9 clusters and a very small amount around the (2,2,2-crypt-K^+) cations. It is important to note, however, that no evidence was found for the presence of en solvent molecules.

All calculations were performed on a 486 personal computer using the SHELXTL PLUS[68] determination package for structure and refinement as well as for structure determination molecular graphics.

Computational Methods. Density functional calculations were done with the program DGauss[69] at the local (LDFT) and nonlocal (NLDFT) (gradient corrected) levels with a basis set in which the Pb core electrons are treated with a pseudopotential[70] (PP) and the valence 6s and 6p electrons are treated with a polarized valence double-ζ basis set. The local potential fit of Vosko, Wilk, and Nusair[54] was used at the local level (VWN/PP). The gradient corrected or nonlocal density functional calculations were done with the nonlocal exchange potential of Becke[55] together with the non-local correlation functional of Perdew (BP/PP).[56] The geometries were optimized by using analytic gradient methods. Second derivatives were calculated by numerical differentiation of the analytic first derivatives. A two point method with a finite difference of 0.01 au was used. All orbital plots were obtained with the UniChem program.

Acknowledgment. We thank the Natural Sciences and Engineering Research Council of Canada for support in the form of a research grant (G.J.S.) and for the award of a graduate scholarship (J.C.).

Supporting Information Available: Text giving procedures of the structure determination and structure determination parameters (Table 7), final atomic coordinates and the equivalent isotropic thermal parameters for the non-hydrogen atoms (Table 8), anisotropic thermal parameters (Table 9), the remaining distances and angles in the (2,2,2-crypt-K^+) cations (Table 11) and atomic coordinates for the hydrogen atoms (Table 12) and stereoviews of the unit cell of K^+(2,2,2-crypt-K^+)$_3Pb_9^{4-}$ (Figure 7a) and (2,2,2-crypt-K^+)$_3Pb_9^{3-}$ (Figure 7b) (30 pages). Ordering information is given on any current masthead page.

IC941320K

(67) Walker, N.; Struat, D. *Acta. Crystallogr.* **1983**, *A39*, 158.
(68) Sheldrick, G. M. SHELXTL PLUS Release 4.21/V. Siemens Analytical X-ray Instruments Inc., Madison, WI, 1990.
(69) (a) Andzelm, J.; Wimmer, E.; Salahub, D. R. *The Challenge of d and f Electrons: Theory and Computation*; Salahub, D. R.; Zerner, M. C., Eds.; ACS Symposium Series 394; American Chemical Society: Washington DC, 1989; pp 228. (b) Andzelm, J., Eds., *Springer-Verlag*, New York, **1991**, pp. 155. (c) Andzelm, J. W.; Wimmer, E. *J. Chem. Phys.* **1992**, *96*, 1280. DGauss is a density functional program available via the Cray Unichem Project.
(70) Chen, H.; Kraskowski, M.; Fitzgerald, G. *J. Chem. Phys.* **1993**, *98*, 8710. (b) Troullier, N.; Martins, J. L. *Phys. Rev. B* **1991**, *43*, 1993.
(71) *International Tables for X-ray Crystallography*; Kynoch Press: Birmingham, England, 1974; Table 5.3.6.B, p 302.